Article

Harnessing the Power of a Novel Triple Chelate Complex in Fermented Probiotic Dairy Products: A Promising Solution for Combating Iron Deficiency Anemia

Alexey Gvozdenko, Andrey Blinov, Alexey Golik, Zafar Rekhman, Andrey Nagdalian, Dionis Filippov, Alina Askerova, Nikita Bocharov, Elena Kastarnova, Faten Abdo Hassan,* Ammar AL-Farga, and Mohammad Ali Shariati*
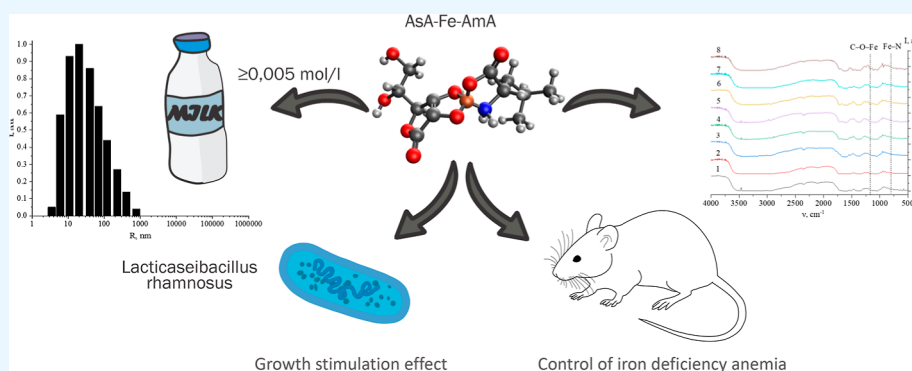
Read Online

ACCESS | Metrics & More | Article Recommendations | Supporting Information

ABSTRACT: This study discovered and examined novel triple chelate complexes involving iron, ascorbic acid, and essential amino acids (AsA-Fe-AmA triple chelate complexes) for the first time. The mechanism of complex formation was studied using FTIR spectroscopy and quantum chemical modeling. The produced complexes were shown to be suitable for fortifying food items with a pH of 3−7 that have not been exposed to heat treatment at temperatures over 75 °C for more than 15 min. Thus, it can be said that the concentration for milk fortification should be 0.005 mol/L or less. In vivo experiments in rats models revealed that the synthesized complexes increased serum iron levels after a single application to reference values within 24 h of oral administration. The iron level increased by 14.0 mmol/L at 2 mL dose of the complex. This fact makes it possible to consider the use of developed complexes and developed fermented dairy products for the prevention of iron deficiency and iron deficiency anemia. Research on the effect of discovered compounds on the physicochemical and organoleptic qualities of milk was conducted. Furthermore, iron ascorbate threoninate, iron ascorbate methioninate, iron ascorbate lysinate, and iron ascorbate tryptophanate all had a beneficial effect on *Lacticaseibacillus rhamnosus* at concentrations as low as 0.0005 mol/L, which is significant for milk fermentation. A study of fermented milk products revealed that the most effective AsA-Fe-AmA triple chelate complex is iron ascorbate lysinate, which might be further investigated as a viable molecule for dietary fortification in iron deficiency anemia. It was found that fortified fermented milk products had a titratable acidity of 67 ± 1°T, pH of 4.38 ± 0.05, and a viscosity of 2018 ± 142 Pa·s.

1. INTRODUCTION

One of the problems of human health is the lack of macro- and microelements in the diet. More than two billion people worldwide have low levels of iron, zinc, iodine, vitamin D, and folic acid.[1−4] Considering that macro- and microelements are necessary for most biological processes in the human body, the lack of these substances can have a significant harmful effect on the physical and mental health of children and adults, and the development of a number of alimentary-dependent diseases (goiter, anemia, rickets, beriberi, Bitot's spots, etc.) can be induced.[5−14]

Nowadays, iron deficiency (ID) stands as the most prevalent condition worldwide.[15,16] ID has a negative impact on

mitochondria.[17,18] Fang et al. demonstrated its particular detrimental effect on the cardiac function, exacerbating heart failure.[19] Neidlein et al. noted that ID reduces the working capacity and muscular strength.[20] According to Pasricha et al.,
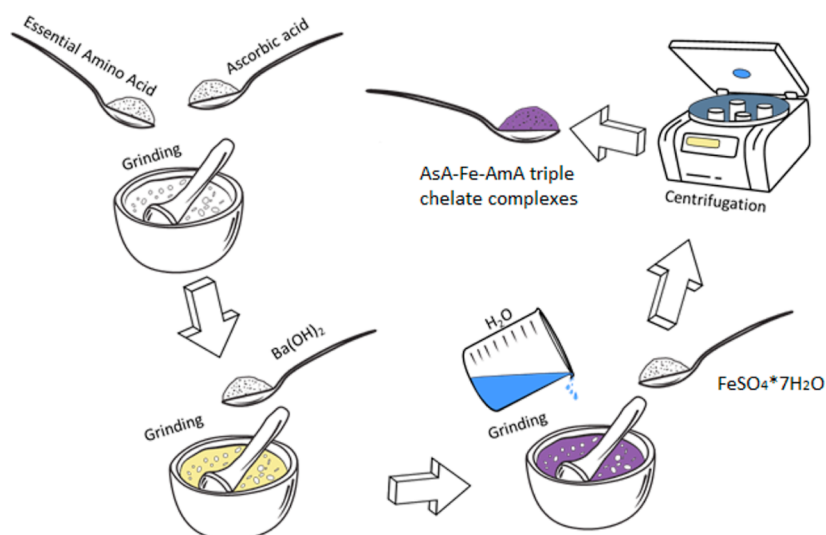
Figure 1. Scheme of the synthesis of triple chelate complexes of the essential trace element iron with ascorbic acid and essential amino acids.

ID can disrupt immunological and endocrine functioning, resulting in the development of iron deficiency anemia (IDA).[21]

Mirza et al. reported that iron deficiency accounts for 50−80% of cases of iron deficiency.[22] IDA is one of the top five causes of disability in women in 35 countries, accounting for many years of impairment.[15,23] According to Garnder et al., the global prevalence of IDA across all ages was 24.3% in 2021, accounting for 1.92 billion prevalent cases, compared to 28.2% and 1.50 billion prevalent cases in 1990. The authors discovered significant disparities in the frequency of IDA across the age, gender, and geography.

According to WHO, IDA affects 53% of children in Africa, 40% in Asia, and 26% in Europe.[24] These figures reported higher than those reported by Stevens et al.[25] in a pooled study of population-representative data spanning from 2000 to 2019. Consequently, the global dynamics of IDA observation are escalating annually. In response, the World Health Assembly Resolution endorsed a Comprehensive implementation plan for maternal, infant, and early child nutrition. This plan delineated a series of nutritional objectives aimed at having the incidence of IDA among women and children twice by 2025.[26,27]

The major strategy for addressing ID and IDA involves supplementing the human diet with bioavailable forms of iron (iron gluconate, iron dextran complex, iron citrate, iron sulfate, iron isomaltoside, etc.).[28−33] Various substances are utilized to enhance the bioavailability of iron. For example, nitrogen alkaloids (piperidine) combined with vitamins and minerals are employed in the production of iron supplements.[34,35] Iron-saccharide compounds have shown excellent efficacy in IDA therapy in model trials with rats.[36,37] However, current research indicates that taking iron complexes orally might have serious side effects.

Thus, Tolkien et al.[38] conducted a meta-analysis of 43 studies, including 6831 adult participants, revealing a significant association between iron sulfate supplementation and gastrointestinal-specific adverse effects. These effects predominantly contain gastrointestinal discomfort such as nausea and vomiting, constipation or diarrhea, flatulence, metallic taste, tooth discoloration, or epigastric pain.[39] As Malesza et al.[40] suggested, iron supplementation can trigger the formation of reactive oxygen species in the gut lumen and enterocytes, leading to an inflammatory process that affects the intestinal wall integrity.

The increase in intestinal wall permeability leads to a complex of unfavorable variables.[41] Excess unabsorbed iron from oral supplementation traverses the colon, where it serves as a critical growth factor for a wide range of pathogenic bacteria, fungi, and protozoa, as well as all neoplastic cells, affecting the gut microbiota considerably.[42,43] Moreover, Moksnes et al.[44] in a genome-wide meta-analysis involving publicly summary statistics covering 257,953 people identified 123 genetic loci associated with iron traits. These loci may be influenced by elevated serum iron and transferrin saturation levels commonly observed with iron supplementation.[45,46]

Iron absorption presents one of the multifactorial adverse effects of oral iron supplementation as documented in the literature.[47] Therefore, the approach to developing bioavailable iron supplements should prioritize innovative methods that optimize iron absorption in order to improve the IDA treatment efficacy and reduce the risk of adverse effects. Ascorbic acid (AsA), citrate, and amino acids (AmA) all help in iron absorption.[48]

AsA enhances iron absorption by converting $Fe(III)$ to $Fe(II)$, facilitating its uptake.[49,50] Noubactep et al.[51] proposed a method to extract iron from granular metallic iron (Fe^0) with AsA, forming a stable and bioavailable $Fe(II)$−AA complex used for drinking water fortification.

Additionally, Cian et al.[52] created microcapsules containing iron and ascorbic acid utilizing chelating polypeptides derived from brewers' waste grain protein. These microcapsules provided high iron bioaccessibility with minimal contact with the food matrix, avoiding redox reactions or adverse effects. Although triple complexes have just recently been explored, they hold significant scientific and practical benefits for producing stable and bioavailable iron formulations.

The aim of this study was to produce and investigate a triple chelate complex of the important trace element iron, ascorbic acid, and essential amino acids (AsA-Fe-AmA) for the development of functional dairy products, particularly milk and fermented dairy items. Milk and dairy products (fermented milk products) offer significant potential for fortification with essential trace elements due to their versatile composition, encompassing both fat and nonfat fractions, enabling the addition of both fat-soluble and water-soluble components. The

resulting fortified fermented milk products can be used to prevent ID and its consequences, in particular, ID anemia.

To the best of our knowledge, these complexes were synthesized for the first time in this study, demonstrating considerable potential for both scientific and practical applications.

2. EXPERIMENTAL DESCRIPTION

2.1. Chemicals and Materials. The study utilized reagent-grade chemicals and grade A glassware. Distilled water with a conductivity of less than 1 μS/cm was used. Dia-M (Moscow, Russia) supplied essential amino acids, such as L-valine, L-leucine, L-isoleucine, L-threonine, L-phenylalanine, L-tryptophan, L-methionine, and L-lysine monohydrochloride. The following chemicals were also purchased for the experiment: ascorbic acid (NeoFroxx, Einhausen, Germany), iron(II) sulfate (Lenreactive, St. Petersburg, Russia), barium hydroxide (Dia-M, Moscow, Russia), potassium persulfate, sulfosalicylic acid (Lenreactive, St. Petersburg, Russia), and 2,2-azinobis(3-ethylbenzothiazoline-6-sulfonic acid) (Alfa Aesar, Ward Hill, MA USA).

The food matrix used was pasteurized with 3.2% fat milk obtained from a local dairy plant (Stavropol Dairy Plant, Stavropol, Russia). *Lacticaseibacillus rhamnosus* and *Lactobacillus acidophilus* strains (Christian Hansen, Hoersholm, Denmark) were employed for fermenting milk products. StavReaChem (Stavropol, Russia) supplied an agar−agar feeding medium for microbiological examination.

2.2. Synthesis of AsA-Fe-AmA Triple Chelate Complexes. The synthesis of AsA-Fe-AmA triple chelate complexes was carried out using our earlier approach,[53] with some minor modifications. In summary, 0.0155 mol of essential amino acids (L-valine, L-leucine, L-isoleucine, L-threonine, L-phenylalanine, L-tryptophan, L-methionine, and L-lysine monohydrochloride) was combined with 0.0155 mol of ascorbic acid. The mixture was then treated with 0.0155 mol of barium hydroxide, 30 mL of distilled water, and 0.0155 mol of iron(II) sulfate. The barium sulfate was extracted from the resultant solution by centrifugation at 3000 rpm using a MicroCL 17R centrifuge (Thermo FS, Waltham, MA, USA). Figure 1 shows the synthesis strategy.

2.3. Characterization of AsA-Fe-AmA Triple Chelate Complexes. The optical properties were studied using an SF-56 spectrophotometer (OKB "Spectrum", St. Petersburg, Russia). For the study, samples of AsA-Fe-AmA triple chelate complexes were diluted 100 times with distilled water. The study parameters were as follows: slit width—6 nm, accumulation time—0.3 s, and wavelength range—400 to 1000 nm.

To investigate the functional groups in the obtained materials, FTIR spectroscopy was performed. IR spectra were acquired on an FSM-1201 IR spectrometer with Fourier transform (Infraspek, St. Petersburg, Russia) across a measuring range of 500−4000 cm^{-1}.

Quantum chemical modeling of AsA-Fe-AmA triple chelate complexes was performed using QChem software and IQmol molecular editor (QChem, Pleasanton, CA, USA) with the following parameters: calculation—energy, technique—HF, basis—6-31G, convergence—5, force field—chemical.

2.4. Stability of AsA-Fe-AmA Triple Chelate Complexes. A multifactorial experiment was carried out to explore the stability of AsA-Fe-AmA triple chelate complexes under various technical parameter values. The input parameters included the medium's active acidity (pH), mixing time (τ, min), and solution temperature (t, °C). The output parameters

were variations in optical density (ΔD). The optical density value was obtained using an SF-56 spectrophotometer (OKB "Spectrum", St. Petersburg, Russia). Table 1 shows the matrix from the multifactorial experiment.

Table 1. Matrix of a Multifactorial Experiment

No.	pH	t, °C	τ, min
1	3	25	5
2	3	60	15
3	3	95	25
4	7	25	15
5	7	60	25
6	7	95	5
7	11	25	25
8	11	60	5
9	11	95	15

2.5. Study of the Effect of AsA-Fe-AmA Triple Chelate Complexes on the Dispersed Composition of Milk. Samples of AsA-Fe-AmA triple chelate complexes were diluted by 10 (concentration: 0.05 mol/L), 100 (concentration: 0.005 mol/L), 1000 (concentration: 0.0005 mol/L), and 10,000 (concentration: 0.00005 mol/L) times with pasteurized milk.

The average hydrodynamic radius of casein micelles in milk was determined using the dynamic light scattering method employing the Photocor Complex device (Photocor, Moscow, Russia), as described in our earlier work.[54] The zeta potential (ζ) and electrical conductivity were measured using an acoustic and electroacoustic spectrometer DT-1202 (Dispersion Technologies, Bedford Hills, NY, USA). Titrated acidity (TA) was calculated using the technique reported by An et al.[55] The pH was determined using an Expert-001 pH meter-ionomer (Econix-Expert, Moscow, Russia) paired with a combination of silver chloride electrode (EVL-1M3.1).

2.6. Investigation of the Antioxidant Activity of Milk Products with AsA-Fe-AmA Triple Chelate Complexes. The antioxidant activity was assessed using the technique reported by Piskov et al.,[56] with slight adjustments. In brief, 5 mL of a 7 mM solution of 2,2-azino bis(3-ethylbenzothiazoline-6-sulfonic acid) (ABTS) and 1 mL of 14.7 mM potassium persulfate were combined and stored at room temperature in the dark for 24 h. Prior to analysis, the ABTS solution was diluted with distilled water to achieve an optical density of 0.70 (±0.02) at λ = 734 nm. Subsequently, 0.25 mL of 0.5 mol/L AsA-Fe-AmA triple chelate complex solution was added to 100 mL of milk. Then, 1 mL of sample and 1 mL of sulfosalicylic acid were centrifuged at 13,000 rpm for 5 min in a MicroCL 17R centrifuge (Thermo FS, Waltham, MA, USA).

The sample was then divided into 0.02 mL aliquots, and to each aliquot 1.98 mL of ABTS solution was added. An SF-56 spectrophotometer (OKB "Spectrum"; St. Petersburg, Russia) was used to detect absorption at 734 nm after 3 min of mixing. 1 mM Trolox solution was employed as a standard. The antioxidant activity was reported in milligrams of Trolox equivalents per mL of sample (mg TE/mL).

2.7. Sensory Analysis. For the sensory study, 10 experimental batches of dairy and fermented milk products were prepared, each comprising 5 samples. Iron(II) sulfate, an inorganic version of the crucial trace element iron, served as the control sample. Following the requirements of ISO 22935−2:2023,[57] a committee of 10 untrained panelists was assembled
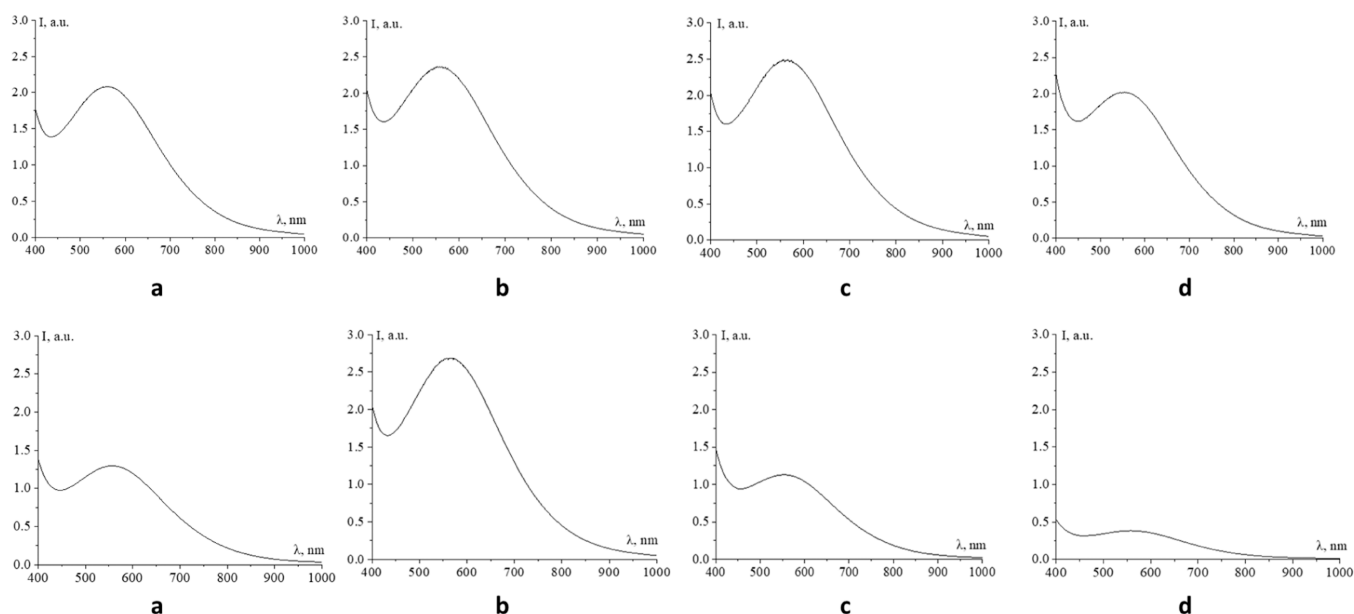
Figure 2. Absorption spectra of triple chelate complexes of the essential trace element iron with ascorbic acid and essential amino acids: a—L-valine, b—L-leucine, c—L-lysine, d—L-threonine, e—L-isoleucine, f—L-methionine, g—L-tryptophan, and h—L-phenylalanine.

to evaluate the sensory attributes of the samples using a 5-point scale.

2.8. Qualitative Microbiological Assessment. *L. rhamnosus* cultured on agar−agar medium was qualitatively assessed following the method described by Alonso-Roman et al.,[58] with minor modifications. To prepare the microbial suspension, the culture was rinsed off with sterile distilled water. The suspension was then filtered through a sterile cotton-gauze filter and diluted with sterile distilled water to a concentration equivalent to 1.0 unit per McFarland standard, which corresponds to 300×106 CFU/mL.

For research purposes, solutions of AsA-Fe-AmA triple chelate complexes were produced at concentrations of 0.05 0.005, 0.0005, and 0.00005 mol/L. *L. rhamnosus* suspensions (100 μL) were inoculated in test tubes containing AsA-Fe-AmA triple chelate complex solutions. Then, they were plated onto Petri dishes with agar−agar and incubated in a thermostat (Binder GmbH, Tuttlingen, Germany) at 37 °C for 24 h. The growing colonies were counted without opening the Petri plates and by flipping them upside down. Each tallied colony was marked with a dot with a fountain pen.

2.9. Production of Fermented Milk Product Fortified with AsA-Fe-AmA Triple Chelate Complexes. Milk fermentation was conducted following the method outlined by Sebastián-Nicolas et al.,[59] with minor modifications. Milk was heated to 95 °C for 1 min. Then, *L. rhamnosus* (1×10^6 CFU), *L. acidophilus* (5×10^6 CFU), and 0.1 mL of 0.5 mol/L AsA-Fe-AmA triple chelate complex solution were added to 150 mL of pasteurized milk. The mixture was stirred and then incubated in a thermostat at 37 °C for 12 h.

2.10. In Vivo Experiment. In the next stage, the effect of triple chelate complexes, specifically iron ascorbate lysinate, on biochemical parameters in the blood of laboratory Wistar rat model of ID anemia was investigated. The ID anemia model was prepared by subcutaneous administration of 0.5 g/kg deferoxamine (Desferal, Novartis Pharma, Switzerland) 2 times with an interval of 3 days.

For a comparative analysis, 6 groups of animals ($n = 5$) were prepared. The first group was kept intact, while the second group

served as a control induced with ID anemia. The third and fourth groups were orally administered with the synthesized complex at a dose of 1 mL/200 g and 2 mL/200 g, respectively. The fifth and sixth groups were intramuscularly administered with Ferran drug (Nita-Pharm, Russia) at doses of 1 mL/200 g and 2 mL/200 g, respectively. Ferran is commonly used in veterinary practice for the treatment of ID anemia. Iron preparations were administered on the 12th day of the experiment. Blood was taken for measurement 24 h after the administration of iron preparations.

Blood for the study was obtained from the heart by piercing the chest wall with a needle with a vacutainer of two types: vacutainer containing an anticoagulant and that containing a gel for separating blood serum. The levels of hemoglobin, erythrocytes, and hematocrit were determined using a Mindray BC-2800 Vet veterinary hematology analyzer (Mindray, Beijing, China). Additionally, the iron content in the blood serum was determined using an automatic biochemical analyzer, a Mindray BS-240 Vet (Mindray, Beijing, China).

2.11. Statistical Data Processing. The biological and analytical studies were repeated three times and five times, respectively. The parameters were analyzed using STATISTICA for Windows (Statsoft, Tulsa, USA) using one-way ANOVA and Student's *t*-test ($p < 0.05$). Microsoft Excel 2010 and Origin software were used to create histograms and graphs based on the collected data.

3. RESULTS AND DISCUSSION

3.1. Optical Properties of AsA-Fe-AmA Triple Chelate Complexes. Initially, the optical characteristics of AsA-Fe-AmA triple chelate complexes were investigated. For the investigation, the samples were 100 times diluted in distilled water. Figure 2 shows the acquired absorption spectra.

The absorption spectra (Figure 2) revealed that all of the generated AsA-Fe-AmA triple chelate complexes exhibited a maximum absorption band in the absorption spectrum between 552 and 567 nm. Table 2 displays the location of the absorption band maximum (λ_{Max}) and the intensity at λ_{Max} (D_{Max}).

Table 2. Optical Properties of AsA-Fe-AmA Triple Chelate Complexes

AsA-Fe-AmA triple chelate complexes	λ_{Max}, nm	D_{Max}, nm
iron ascorbate valinate	559	2.0836
iron ascorbate lysinate	567	2.4969
iron ascorbate leucinate	552	2.3656
iron ascorbate threoninate	554	2.0221
iron ascorbate isoleucinate	557	1.2961
iron ascorbate methioninate	567	2.6919
iron ascorbate tryptophanate	554	1.1281
iron ascorbate phenylalaninate	552	0.4324

Analysis of the data presented in Figure 2 and Table 2 revealed that the amino acid in the complexes' composition influences the location of maximal absorption of the AsA-Fe-AmA triple chelate complex. Specifically, iron ascorbate isoleucinate and phenylalaninate had the lowest λ_{max} (552 nm), while ascorbate methioninate and iron ascorbate lysinate had the highest λ_{max} (567 nm). However, a narrow range of 552–567 nm can be attributed to the closely comparable rate of iron concentration and saturation.[60,61]

3.2. Characterization of AsA-Fe-AmA Triple Chelate Complex Formation. The formation of AsA-Fe-AmA triple chelate complexes was initially explored through computed quantum chemical modeling. Various models were examined, considering the potential formation of a triple chelate complex via amino and carboxyl groups or amino and hydroxyl groups of AmA, as well as hydroxyl groups attached to ascorbic acid's C2, C3, C5, or C6 carbon atoms. Table 3 shows the total energy and chemical rigidity values obtained for the molecular complexes under investigation.

Computed quantum chemical modeling revealed that the molecule complex models are not only energetically favorable but also chemically stable ($0.058 < \eta < 0.113$ eV).[62] The interaction between AmA and AsA was found to occur through the amino and carboxyl groups of AmA and hydroxyl groups attached to C2 and C3 carbon atoms of AsA (Figure 3). This configuration was favored due to its minimal total value energy compared to other configurations.[63,64]

The Supporting Information (Figures S1–S60) contains models of molecular complexes, electron density distributions, electron density distribution gradients, and visualizations of the highest occupied molecular orbital (HOMO) and lowest occupied molecular orbital (LUMO) of AsA-Fe-AmA triple chelate complexes.

To validate the results of computed quantum chemical modeling on AsA-Fe-AmA triple chelate complexes, FTIR spectroscopy was employed. Figures 4 and S61–S62 exhibit the acquired data.

The IR spectra of AsA-Fe-AmA triple chelate complexes (Figure 4) revealed valence variations for the $-CO_2^-$, NH_3^+, OH, CH_2, and CH_3 groups between 2500 and 3500 cm^{-1}. Additionally, the infrared spectra show bands typical for AsA: the bands at 634, 719, and 1755 cm^{-1} correspond to vibrations of C=O; the band at 1670 cm^{-1} corresponds to vibrations of C=C in the C2 and C3 atoms of AsA; the bands at 1498, 1365, 1197, and 990 cm^{-1} correspond to the deformation vibrations of the CH_2 group.[65,66] Furthermore, up to 1300 cm^{-1}, there are deformation variations of $-CH_2$ and $-CH_3$ groups, which are typical of AmA.[67]

It is worth noting that the IR spectra of AsA-Fe-AmA chelate complexes show a decrease in the strength of a number of bands.

- AmA's NH_3^+ group deformation vibrations occur in the 1485–1550 cm^{-1} range; $-COO^-$ group vibrations occur in the 1300–1330 cm^{-1} range;
- AsA's C–OH group deformation vibrations occur at 1278 and 1448 cm^{-1}; $-$AsA's C–OH group deformation vibrations occur at 1330 cm^{-1}.

The analysis of the IR spectra showed bands that are not indicative of AsA or AmA:

- 1160–1170 cm^{-1} corresponds to C–O–Fe variations;[68]
- the wavelength range 795–805 cm^{-1} corresponds to Fe–N variations.[69]

Consequently, the AsA-Fe-AmA triple chelate complexes are formed via the AsA OH group and AmA COO$^-$ and NH$_3^+$ groups, respectively. The interaction between Fe and the OH group of AsA results in the formation of a C–O–Fe bond in the 1160–1170 cm^{-1} range and a decrease in the intensity of bands of C–O–H (1278 and 1448 cm^{-1}) and C–OH (1330 cm^{-1}).

It was discovered that the interaction between Fe and the COO$^-$ group of AmA results in the production of a C–O–Fe bond in the range of 1160–1170 cm^{-1} accompanied by a reduction in the strength of the COO$^-$ group band (1300–1330 cm^{-1}). Simultaneously, the interaction between Fe and the NH$_3^+$ group of AmA results in the production of a Fe–N bond in the range 795–805 cm^{-1}, along with a decrease in the intensity of the NH$_3^+$ group's deformation vibration band (1485–1550 cm^{-1}). Figure 8 depicts the formation of triple chelate complexes of the necessary trace metals iron, ascorbic acid, and essential amino acids.

Hence, the FTIR spectroscopy results are consistent with computed quantum chemical modeling. Drawing from these findings, a technique for the creation of AsA-Fe-AmA triple chelate complexes was devised and is illustrated in Figure 5.

3.3. Stability of AsA-Fe-AmA Triple Chelate Complexes. In addition to comprehending the formation process of AsA-Fe-AmA triple chelate complexes, it is critical to understand their stability. To achieve this, a multifactorial experiment was conducted, incorporating three input parameters: pH, temperature (T), and exposure period. The output parameter was specified as the change in optical density (ΔD)

$$\Delta D = D_0 - D_{pH, T, \tau} \tag{1}$$

where

D_0: value of the optical density at λ_{Max} in the absorption spectrum of the complex after formation.

$D_{pH, T, \tau}$: value of the optical density at t λ_{Max} in the absorption spectrum of the complex at given values of pH, T, and τ.

The collected data underwent mathematical and statistical analyses, as illustrated in Figure 9 and Supporting Information, which display the obtained dependencies. The examination of the acquired dependencies revealed that the stability of AsA-Fe-AmA triple chelate complexes is significantly influenced by all of the studied factors. Increases in pH, T, and τ lead to an increase in ΔD, indicating complicated decay. Conversely, the highest ΔD values were recorded at pH = 8–11, T = 75–95 °C, and τ = 20–25 min. The lowest ΔD values were found at pH = 3–7, T = 20–75 °C, and τ = 5–15 min, indicating the complexes' stability in this range of parameters (Figures 6 and S63–S69).[69]

Table 3. Results of Computed Quantum Chemical Calculations

amino acid	groups of amino acid	carbon atoms in ascorbic acid attached with hydroxyl groups	E, kcal/mol	E_{HOMO}, eV	E_{LUMO}, eV	η, eV
L-valine	amino and carboxyl groups	C2 and C3	−2338.360	−0.131	0.025	0.078
		C2 and C6	−2338.128	−0.177	0.041	0.109
		C2 and C5	−2338.144	−0.114	0.045	0.080
		C3 and C6	−2338.140	−0.110	0.052	0.081
		C3 and C5	−2338.127	−0.089	0.056	0.073
		C5 and C6	−2338.082	−0.082	0.065	0.074
L-leucine	amino and carboxyl groups	C2 and C3	−2377.402	−0.142	0.026	0.084
		C2 and C6	−2377.021	−0.154	0.042	0.098
		C2 and C5	−2377.204	−0.105	0.035	0.070
		C3 and C6	−2377.010	−0.186	0.018	0.102
		C3 and C5	−2377.124	−0.095	0.053	0.074
		C5 and C6	−2377.080	−0.077	0.067	0.072
L-isoleucine	amino and carboxyl groups	C2 and C3	−2377.365	−0.129	0.015	0.072
		C2 and C6	−2377.142	−0.175	0.042	0.109
		C2 and C5	−2377.137	−0.102	0.036	0.069
		C3 and C6	−2377.162	−0.110	0.054	0.082
		C3 and C5	−2377.078	−0.096	0.041	0.069
		C5 and C6	−2377.083	−0.084	0.069	0.077
L-methionine	amino and carboxyl groups	C2 and C3	−2735.826	−0.141	0.030	0.086
		C2 and C6	−2735.510	−0.163	0.010	0.087
		C2 and C5	−2735.674	−0.119	0.025	0.072
		C3 and C6	−2735.536	−0.178	0.010	0.094
		C3 and C5	−2735.590	−0.105	0.047	0.076
		C5 and C6	−2735.532	−0.081	0.064	0.073
L-threonine	amino and carboxyl groups	C2 and C3	−2374.162	−0.133	0.021	0.077
		C2 and C6	−2373.917	−0.193	0.032	0.113
		C2 and C5	−2374.027	−0.111	0.024	0.068
		C3 and C6	−2373.923	−0.111	0.045	0.078
		C3 and C5	−2373.924	−0.100	0.048	0.074
		C5 and C6	−2373.933	−0.079	0.057	0.068
	amino and hydroxyl groups	C2 and C3	−2374.157	−0.129	0.025	0.077
		C2 and C6	−2373.836	−0.156	0.010	0.083
		C2 and C5	−2373.979	−0.103	0.040	0.072
		C3 and C6	−2373.884	−0.164	0.021	0.093
		C3 and C5	−2373.946	−0.98	0.023	0.061
		C5 and C6	−2373.956	−0.78	0.060	0.069
L-lysine	amino and carboxyl groups	C2 and C3	−2432.391	−0.145	0.039	0.092
		C2 and C6	−2431.841	−0.184	0.027	0.106
		C2 and C5	−2432.146	−0.096	0.046	0.071
		C3 and C6	−2432.074	−0.170	0.022	0.096
		C3 and C5	−2432.152	−0.110	0.032	0.071
		C5 and C6	−2432.084	−0.079	0.084	0.082
	amino and hydroxyl groups	C2 and C3	−2432.033	−0.125	0.045	0.085
		C2 and C6	−2431.950	−0.141	0.083	0.112
		C2 and C5	−2432.073	−0.083	0.075	0.079
		C3 and C6	−2432.079	−0.086	0.061	0.074
		C3 and C5	−2432.070	−0.076	0.069	0.073
		C5 and C6	−2432.060	−0.054	0.080	0.067
L-phenylalanine	amino and carboxyl groups	C2 and C3	−2489.802	−0.138	0.043	0.091
		C2 and C6	−2489.457	−0.156	0.030	0.093
		C2 and C5	−2489.521	−0.096	0.034	0.065
		C3 and C6	−2489.189	−0.173	0.004	0.089
		C3 and C5	−2489.514	−0.091	0.052	0.072
		C5 and C6	−2489.502	−0.075	0.067	0.071
L-tryptophan	amino and carboxyl groups	C2 and C3	−2620.485	−0.128	0.047	0.088
		C2 and C6	−2620.146	−0.170	0.037	0.104
		C2 and C5	−2620.303	−0.114	0.025	0.070
		C3 and C6	−2620.246	−0.103	0.050	0.077
		C3 and C5	−2620.281	−0.087	0.055	0.071
		C5 and C6	−2620.165	−0.070	0.046	0.058
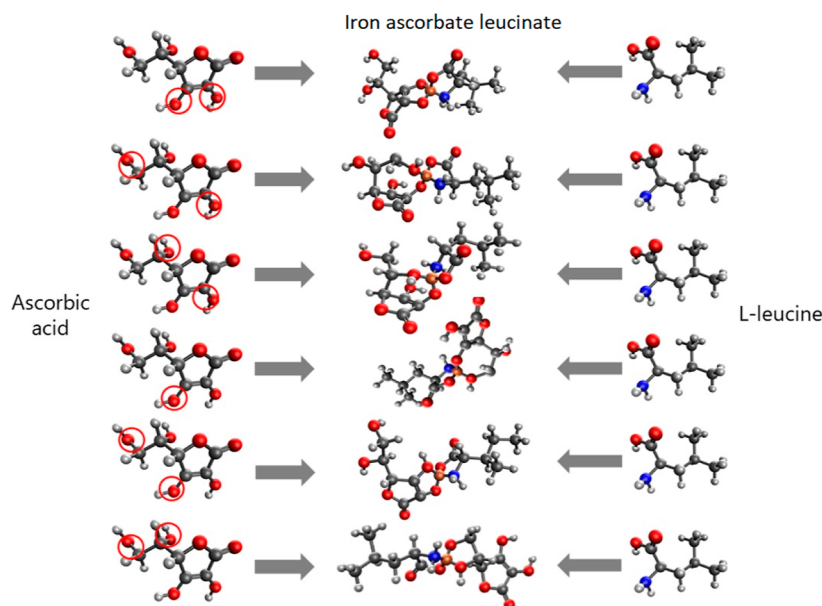
Figure 3. Possible variants of the AsA-Fe-AmA triple chelate complex formation with an example of iron ascorbate leucinate (hydroxyl groups involved in the complex formation are marked by circles).
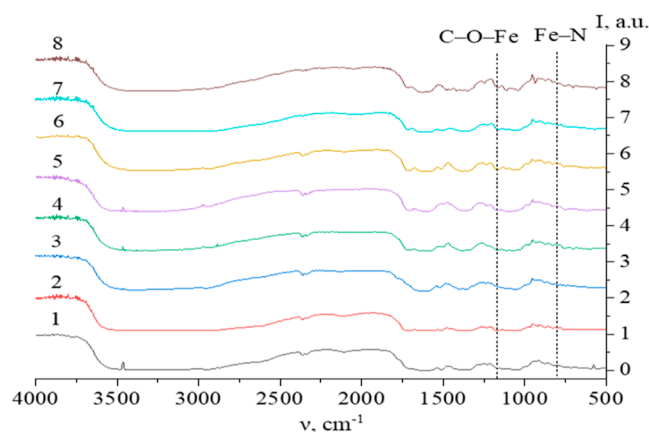
Figure 4. IR spectra of AsA-Fe-AmA triple chelate complexes: 1—L-valine, 2—L-isoleucine, 3—L-leucine, 4—L-phenylalanine, 5—L-tryptophan, 6—L-methionine, 7—L-lysine, and 8—L-threonine.

Analysis of these dependencies revealed that the stability of the AsA-Fe-AmA triple chelate complexes is significantly influenced by all of the factors investigated. Increases in pH, temperature (T), and exposure period (τ) lead to an increase in ΔD, indicating complex decay processes. The highest ΔD values were recorded at pH = 8−11, T = 75−95 °C, and τ = 20−25 min. Conversely, the lowest ΔD values were found at pH = 3−7, T = 20−75 °C, and τ = 5−15 min, indicating greater stability of the complexes within this parameter range (Figures 6 and S63−S69).

Thus, it can be concluded that the newly synthesized AsA-Fe-AmA triple chelate complexes are appropriate for fortification of food items with a pH range of 3−7 and have not been exposed to heat treatment at temperatures over 70 °C for more than 15 min. Pasteurized milk and fermented dairy products derived from it (kefir, ryazhenka, yogurt, etc.) were identified as a suitable food matrix that could be included in a daily diet, as supported by multiple recent studies.[70−72] However, these compounds may have a considerable impact on the stable dispersion system of milk and fermented dairy products.[73−75] As a result, the effect of
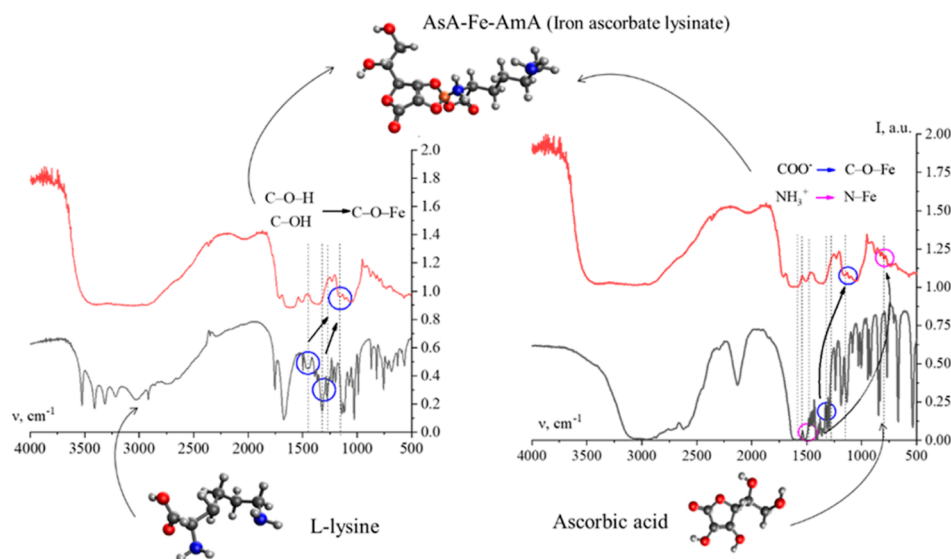
AsA-Fe-AmA triple chelate complexes on the distributed content of milk should be thoroughly investigated.

3.4. In Vivo Experiment. In the next stage, the effect of triple chelate complexes, in particular, iron ascorbate lysinate, on the biochemical parameters of the blood of laboratory Wistar rats was investigated. The results are presented in Table 4.

Table 4 shows that the level of hemoglobin, erythrocytes, and hematocrit in all groups did not differ statistically. Notably, according to the literature data, blood parameters of laboratory animals (hemoglobin, erythrocyte, and hematocrit levels) should recover in 30 days.[76,77] At the same time, serum iron values after a single application of AsA-Fe-AmA reached reference values within 24 h after administration. There was a statistically significant difference in the level of iron in the blood of laboratory rats. After administration of AsA-Fe-AmA, the iron level increased by 10.7 and 14.0 mmol/L in groups 3 and 4, respectively, compared to the control group. Notably, AsA-Fe-AmA increased the iron level in blood by 1.5 mmol/L (group 3) and 3.8 mmol/L (group 4) compared with that of the intact group without ID anemia. Moreover, there were no statistical differences between the effects of AsA-Fe-AmA and Ferran drug, which is commonly used in veterinary practice for the treatment of ID anemia. Thus, AsA-Fe-AmA balanced the iron level in the blood of laboratory rat model with ID anemia within 24 h of oral administration, which is compared with the effectiveness of commercial drugs.

3.5. Effect of AsA-Fe-AmA Triple Chelate Complexes on the Dispersed Composition of Milk. Table 5 shows the effects of AsA-Fe-AmA triple chelate complexes on milk's dispersed composition, encompassing parameters such as TA, electrical conductivity (δ), pH, average hydrodynamic radius (R), and zeta potential (ζ) at various complex concentrations.

According to Table 5, 0.05 mol/L AsA-Fe-AmA triple chelate complexes induced the coagulation of milk proteins, leading to the separation and precipitation of milk fractions. At this concentration, samples with iron ascorbate valinate had the most significant increase in the average hydrodynamic radius of casein micelles (980 vs 30 nm in the control sample). Samples with iron ascorbate tryptophanate had the highest TA of 55°T

Figure 5. Scheme for the formation of AsA-Fe-AmA triple chelate complexes with an example of iron ascorbate lysinate.
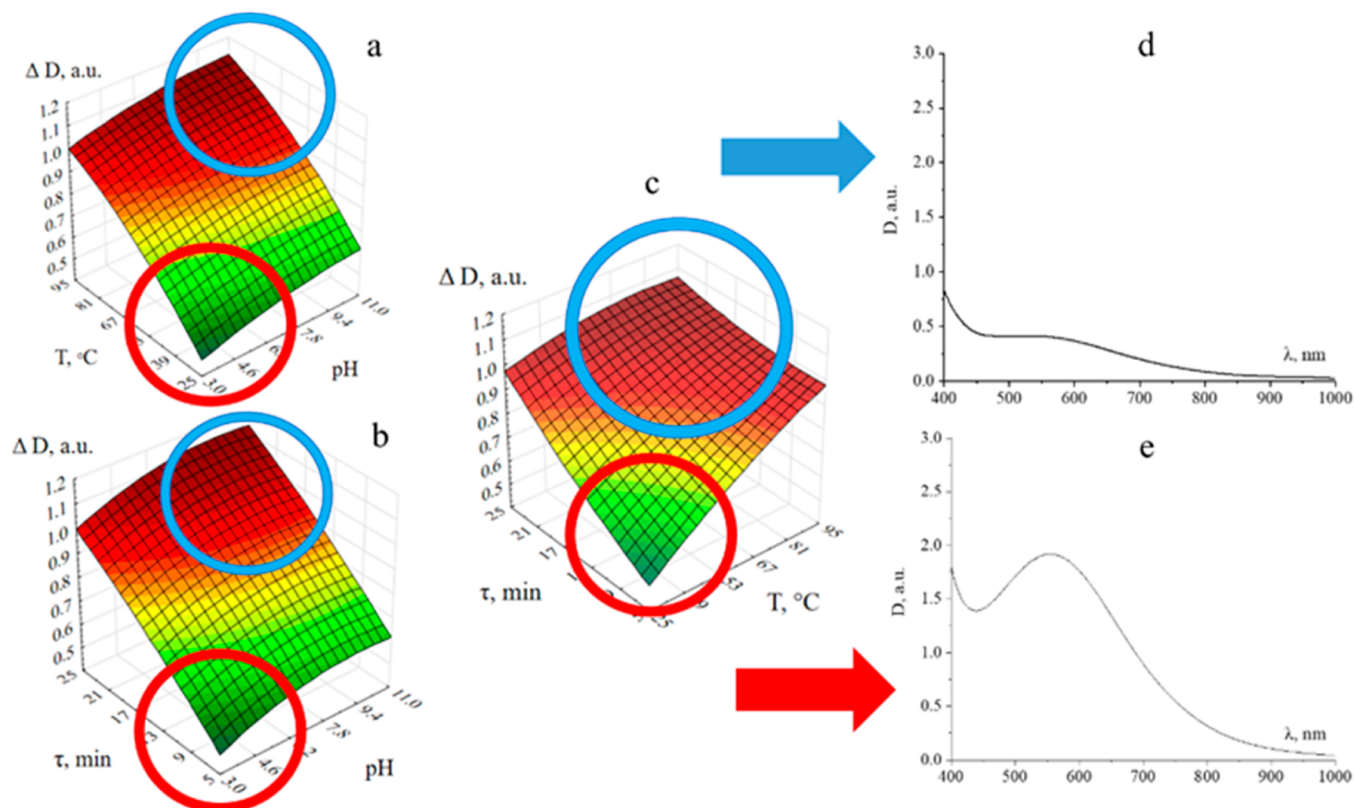
Figure 6. Stability assessment of AsA-Fe-AmA triple chelate complexes: dependences of changes in the optical density on pH and T (a), pH and τ (b), and T and τ (c); absorption spectra of samples in the region with the largest change in optical density (d) and with the smallest change in optical density (e) (iron ascorbate lysinate).

(18°T in the control sample) and the lowest pH (5.42 vs 6.78 in the control sample). Electrical conductivity and zeta potential remained stable. Figure 7 depicts a histogram of the average hydrodynamic radius of casein micelles in milk samples with 0.05 mol/L iron ascorbate valinate. It is noteworthy that the similar tendency of casein micelle growth was reported in our earlier study on milk fortification with zinc lysinate riboflavinate at concentrations greater than 0.05 mol/L.[78]

At concentrations of 0.005, 0.0005, and 0.00005 mol/L, the samples exhibited no significant alterations. Casein micelles maintained an average hydrodynamic radius of 27−79 nm, a TA of 17−21 °T, and a pH range of 6.66−6.80. The electrical conductivity and zeta -potential remained stable. Figure 8 depicts a histogram of the average hydrodynamic radius of casein micelles in milk samples with 0.005 mol/L of iron ascorbate valinate.

Table 4. Biochemical Parameters of Blood of Laboratory Rat Model with ID Anemia

index	experimental groups					
	group 1 (intact)	group 2 (control with ID anemia)	group 3 (1 mL/200 g AsA-Fe-AmA)	group 4 (2 mL/200 g AsA-Fe-AmA)	group 5 (1 mL/200 g Ferran)	group 6 (2 mL/200 g Ferran)
hemoglobin, g/L	16.19 ± 0.51	10.43 ± 0.48	10.65 ± 0.50	10.48 ± 0.48	10.42 ± 0.51	10.46 ± 0.54
erythrocytes, × 10^{12}/L	11.60 ± 0.14	7.45 ± 0.50	7.47 ± 0.48	7.43 ± 0.51	7.46 ± 0.49	7.45 ± 0.47
hematocrit,%	35.25 ± 1.15	23.19 ± 0.93	23.24 ± 0.87	23.15 ± 0.76	23.42 ± 0.77	23.31 ± 0.80
Fe, mmol/L	26.3 ± 0.8	16.1 ± 1.3	27.8 ± 1.0	30.1 ± 0.9	26.0 ± 1.1	28.9 ± 1.2
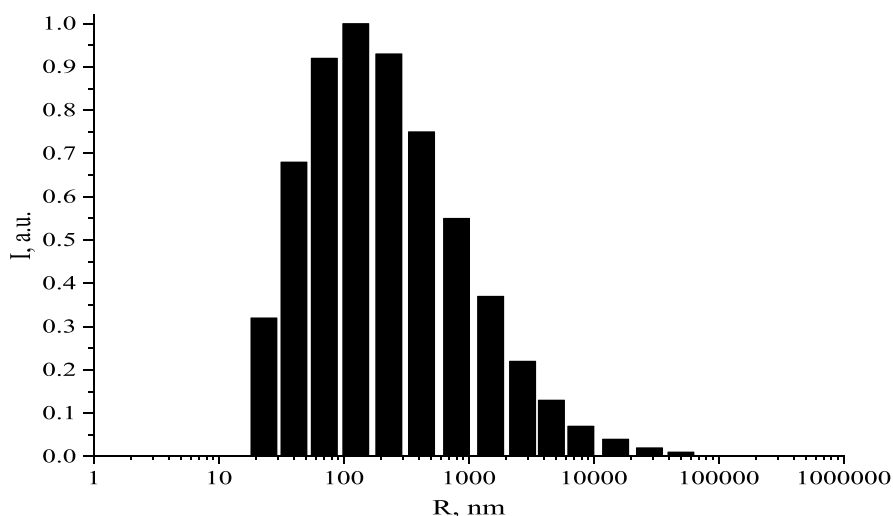
Figure 7. Histogram of the average hydrodynamic radius of casein micelles in milk samples with 0.05 mol/L iron ascorbate valinate.
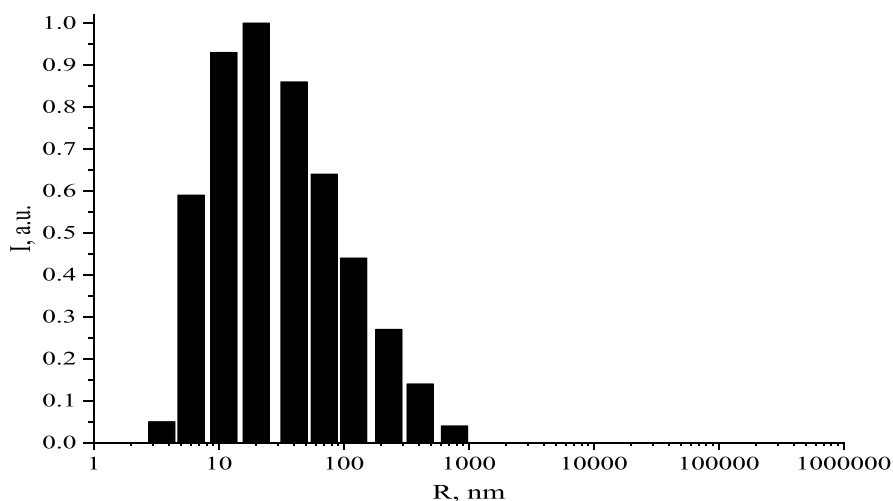
Figure 8. Histogram of the average hydrodynamic radius of casein micelles in milk samples with 0.005 mol/L iron ascorbate valinate.

The analysis of the acquired data revealed that milk should be fortified with AsA-Fe-AmA triple chelate complexes at concentrations of 0.005 mol/L or less, corresponding to a dilution of 1:100 or less (Figure 9).

3.6. Antioxidant Activity and Sensory Properties of Milk Fortified with AsA-Fe-AmA Triple Chelate Complexes. In the subsequent stage of the experiment, the antioxidant activity (AoA) of the fortified milk was investigated. The data obtained are presented in Table 6.

Table 6 demonstrates that AsA-Fe-AmA triple chelate complexes improved the AoA of enriched milk samples. The most significant impact was found with the use of iron ascorbate

phenylalaninate (0.92 mg TE/mL), while the lowest effect was noted with the use of iron ascorbate threoninate (0.53 mg TE/mL), still surpassing the AoA value in the control sample (0.30 mg TE/mL). Interestingly, iron ascorbate phenylalaninate exhibited a higher amount of AoA than AsA. These results align with the well-known AoA of AsA and AmA and their efficacy in milk fortification.[79−81]

Iron complexes are known to significantly influence the sensory qualities of milk and dairy products, which warrants further investigation. García et al.[82] reported that iron fortification at different concentrations markedly affected the sensory acceptability of milk. Abdulghani et al.[83] observed the

Table 5. Effect of AsA-Fe-AmA Triple Chelate Complexes on the Dispersed Composition of Milk[a]

concentration, mol/L	parameters	iron ascorbate lysinate	iron ascorbate leucinate	iron ascorbate isoleucinate	iron ascorbate valinate	iron ascorbate phenylalaninate	iron ascorbate threoninate	iron ascorbate tryptophanate	iron ascorbate methioninate
0.05	R, nm[b]	314 ± 20	248 ± 22	429 ± 37	988 ± 78	132 ± 12	441 ± 34	89 ± 9	381 ± 34
	δ, S[b]	0.40 ± 0.5	0.94 ± 0.5	0.77 ± 0.5	0.99 ± 0.5	1.00 ± 0.5	1.15 ± 0.5	1.08 ± 0.5	0.81 ± 0.5
	ζ, mV[b]	−1.08 ± 1.00	−0.48 ± 1.00	1.07 ± 1.00	−1.04 ± 1.00	−0.97 ± 1.00	−0.44 ± 1.00	−1.91 ± 1.00	−0.2 ± 1.00
	pH[b]	6.62 ± 0.05	6.45 ± 0.05	6.44 ± 0.05	6.47 ± 0.05	6.12 ± 0.05	6.01 ± 0.05	5.42 ± 0.05	6.48 ± 0.05
	TA, °T[b]	27 ± 1	28 ± 1	24 ± 1	35 ± 1	32 ± 1	37 ± 1	55 ± 1	40 ± 1
0.005	R, nm	44 ± 5	45 ± 5	49 ± 5	69 ± 6	50 ± 5	51 ± 5	50 ± 5	79 ± 7
	δ, S	0.70 ± 0.5	0.70 ± 0.5	0.74 ± 0.5	0.94 ± 0.5	1.39 ± 0.5	0.93 ± 0.5	0.76 ± 0.5	0.92 ± 0.5
	ζ, mV	−0.39 ± 1.00	0.3 ± 1.00	−0.45 ± 1.00	−0.26 ± 1.00	−0.56 ± 1.00	−0.27 ± 1.00	−0.44 ± 1.00	0.32 ± 1.00
	pH	6.68 ± 0.05	6.66 ± 0.05	6.69 ± 0.05	6.75 ± 0.05	6.7 ± 0.05	6.73 ± 0.05	6.76 ± 0.05	6.76 ± 0.05
	TA, °T	19 ± 1	19 ± 1	20 ± 1	17 ± 1	19 ± 1	20 ± 1	19 ± 1	18 ± 1
0.0005	R, nm	36 ± 4	31 ± 4	38 ± 4	49 ± 5	36 ± 4	37 ± 4	35 ± 4	41 ± 4
	δ, S	0.91 ± 0.5	0.80 ± 0.5	0.79 ± 0.5	0.76 ± 0.5	1.02 ± 0.5	2.03 ± 0.5	0.79 ± 0.5	0.71 ± 0.5
	ζ, mV	0.23 ± 1.00	−0.94 ± 1.00	−0.93 ± 1.00	0.14 ± 1.00	0.52 ± 1.00	0.42 ± 1.00	−0.70 ± 1.00	−0.84 ± 1.00
	pH	6.76 ± 0.05	6.76 ± 0.05	6.75 ± 0.05	6.78 ± 0.05	6.73 ± 0.05	6.75 ± 0.05	6.74 ± 0.05	6.8 ± 0.05
	TA, °T	19 ± 1	19 ± 1	20 ± 1	17 ± 1	19 ± 1	20 ± 1	19 ± 1	18 ± 1
0.00005	R, nm	31 ± 3	28 ± 3	32 ± 3	33 ± 3	36 ± 4	31 ± 3	29 ± 3	31 ± 3
	δ, S	0.73 ± 0.5	0.74 ± 0.5	0.85 ± 0.5	0.78 ± 0.5	0.85 ± 0.5	1.77 ± 0.5	0.92 ± 0.5	1.03 ± 0.5
	ζ, mV	−0.77 ± 1.00	0.85 ± 1.00	0.66 ± 1.00	0.61 ± 1.00	0.45 ± 1.00	0.39 ± 1.00	−1.36 ± 1.00	0.75 ± 1.00
	pH	6.77 ± 0.05	6.78 ± 0.05	6.76 ± 0.05	6.79 ± 0.05	6.80 ± 0.05	6.75 ± 0.05	6.77 ± 0.05	6.79 ± 0.05
	TA, °T	21 ± 1	17 ± 1	18 ± 1	17 ± 1	17 ± 1	18 ± 1	20 ± 1	18 ± 1
control	R, nm	30 ± 2							
	δ, S	0.78 ± 0.5							
	ζ, mV	−0.52 ± 1.00							
	pH	6.78 ± 0.05							
	TA, °T	18 ± 1							

[a]R—average hydrodynamic radius, δ—electrical conductivity, TA—titrated acidity. [b]X ± standard error of device (N = 3).
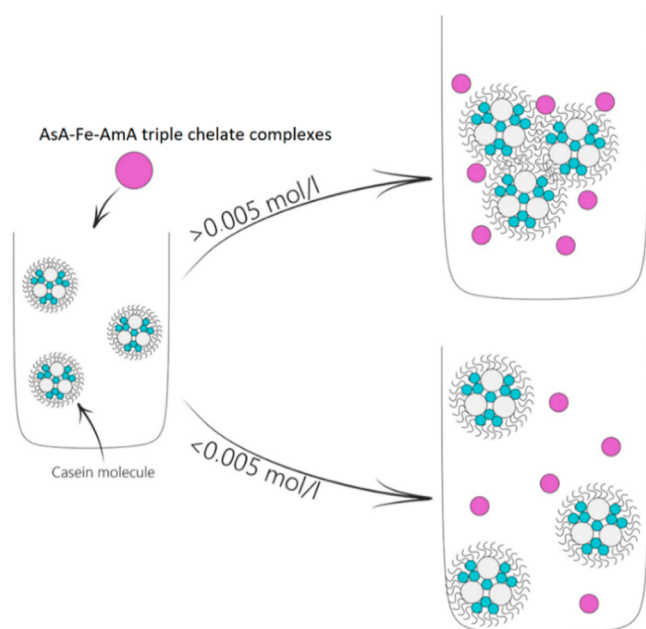
Figure 9. Scheme of the effect of AsA-Fe-AmA triple chelate complexes on casein micelles.

same outcomes. Siddique and Park[84] produced and tested cheese enriched with ordinary ferrous sulfate and big micro-encapsulated ferrous sulfate. While the iron-fortified cheese exhibited improved functional and structural qualities, it received lower taste ratings, posing a challenge for industrial production. Arce and Ustunol[85] also found that iron-fortified cheese displayed poor sensory characteristics, rating lower than control samples in appearance, texture, taste, and overall acceptability.

Hence, iron fortification of milk might result in considerable changes in sensory characteristics, decreasing its acceptability. Thus, the sensory study of milk enriched with AsA-Fe-AmA triple chelate complexes was critical. Table 7 presents the sensory evaluation results.

The sensory evaluation revealed that milk samples fortified with iron(II) sulfate, iron ascorbate tryptophanate, and iron ascorbate phenylalaninate had a clean, pleasant, and slightly sweet taste and odor. However, milk samples fortified with other AsA-Fe-AmA triple chelate complexes had changes in taste and odor, resulting in lower overall sensory acceptability scores. Consequently, iron ascorbate tryptophanate and iron ascorbate phenylalaninate were identified as the best complexes for milk

fortification based on sensory acceptability. They might warrant further investigation as a viable substance for food fortification in iron deficiency anemia.

3.7. Effect of AsA-Fe-AmA Triple Chelate Complexes on Lactic Acid Bacteria. Recent studies have demonstrated the antibacterial activity of iron complexes used for milk fortification. For instance, Helmyati et al.[86] fortified milk with NaFeEDTA and FeSO$_4$ and recorded the antibacterial action against *E. coli* and *S. aureus*, as well as a reduction in total Enterobacteriaceae over a four week monitoring period. Similarly, Harouna et al.[87] found iron-saturated bovine lactoferrin reduced the viability of C. sakazakii in whey. Consequently, when fermented dairy products from milk enriched with AsA-Fe-AmA triple chelate complexes are produced, it is critical to understand how these complexes interact with bacteria, as their antibacterial impact may inhibit milk fermentation. To investigate the effect of AsA-Fe-AmA triple chelate complexes on lactic acid bacteria, solutions of complexes were prepared at concentrations of 0.05 mol/L (A), 0.005 mol/L (B), 0.0005 mol/L (C), and 0.00005 mol/L (D) for research purposes. Subsequently, 100 μL *L. rhamnosus* suspensions were added to test tubes with AsA-Fe-AmA triple chelate complexes solutions and plated on Petri dishes with agar−agar. The Petri dishes were then placed in a thermostat (Binder GmbH, Tuttlingen, Germany) at 37 °C for 24 h. The acquired photos of Petri dishes are shown in Figure 10.

The CFU value was determined for all samples and is presented in Table 8.

According to the findings in Table 8, the concentration and type of AsA-Fe-AmA triple chelate complexes exert a substantial impact on the growth and development of *L. rhamnosus* lactic acid cultures. However, at a concentration of 0.05 mol/L, CFU varies from 0.75×10^6 to 0.82×10^6 in 1 mL, with no significant difference between them. At a concentration of 0.005 mol/L, CFU varies from 0 to 1.56×10^6 per mL. Iron ascorbate valinate was the sole complex that had a detrimental influence on the growth and development of *L. rhamnosus*. Notably, decreasing quantities of iron ascorbate threoninate, iron ascorbate lysinate, iron ascorbate leucinate, and iron ascorbate isoleucinate resulted in an increase in the CFU value.

Similarly, iron ascorbate methioninate, iron ascorbate phenylalaninate, and iron ascorbate tryptophanate showed no significant influence on the concentration. At 0.0005 mol/L, iron ascorbate threoninate, iron ascorbate methioninate, iron ascorbate lysinate, and iron ascorbate tryptophanate improved the growth and development of *L. rhamnosus* compared to the control sample. The findings are significant, as the complexes

Table 6. Antioxidant Activity of Milk Fortified with AsA-Fe-AmA Triple Chelate Complexes

samples	D (blank sample), au	D (sample), au	AoA, %	AoA, mg TE/mL
milk with iron ascorbate lysinate	0.700	0.638	17.7	0.66
milk with iron ascorbate phenylalaninate	0.694	0.609	24.5	0.92
milk with iron ascorbate isoleucinate	0.697	0.628	19.8	0.74
milk with iron ascorbate tryptophanate	0.707	0.645	17.5	0.66
milk with iron ascorbate methioninate	0.697	0.645	14.9	0.56
milk with iron ascorbate valinate	0.704	0.645	16.8	0.63
milk with iron ascorbate threoninate	0.702	0.652	14.2	0.53
milk with iron ascorbate leucinate	0.727	0.675	14.7	0.55
ascorbic acid	0.713	0.640	20.3	0.76
1 mg Trolox	0.727	0.533	26.7	1
control milk sample	0.731	0.702	7.9	0.30

Table 7. Sensory Characteristics of Milk Fortified with AsA-Fe-AmA Triple Chelate Complexes

sample	general description	total value[a]
milk with iron(II) sulfate	clean, pleasant, slightly sweet	4.81
milk with iron ascorbate lysinate	slightly pronounced unclean, foreign smell and taste	4.40
milk with iron ascorbate valinate	slightly pronounced unclean, foreign smell and taste	3.18
milk with iron ascorbate isoleucinate	slightly pronounced unclean, foreign smell and taste	3.63
milk with iron ascorbate threoninate	insufficiently pronounced, empty, without foreign odors and flavors	3.96
milk with iron ascorbate methioninate	pronounced unclean, peculiar smell, salty taste	2.83
milk with iron ascorbate tryptophanate	clean, pleasant, slightly sweet	4.70
milk with iron ascorbate phenylalaninate	clean, pleasant, slightly sweet	4.65
milk with iron ascorbate leucinate	insufficiently pronounced, empty, without foreign odors and flavors	4.02
control milk sample	clean, pleasant, slightly sweet	4.81

[a]Weighted average value ($N = 10$).
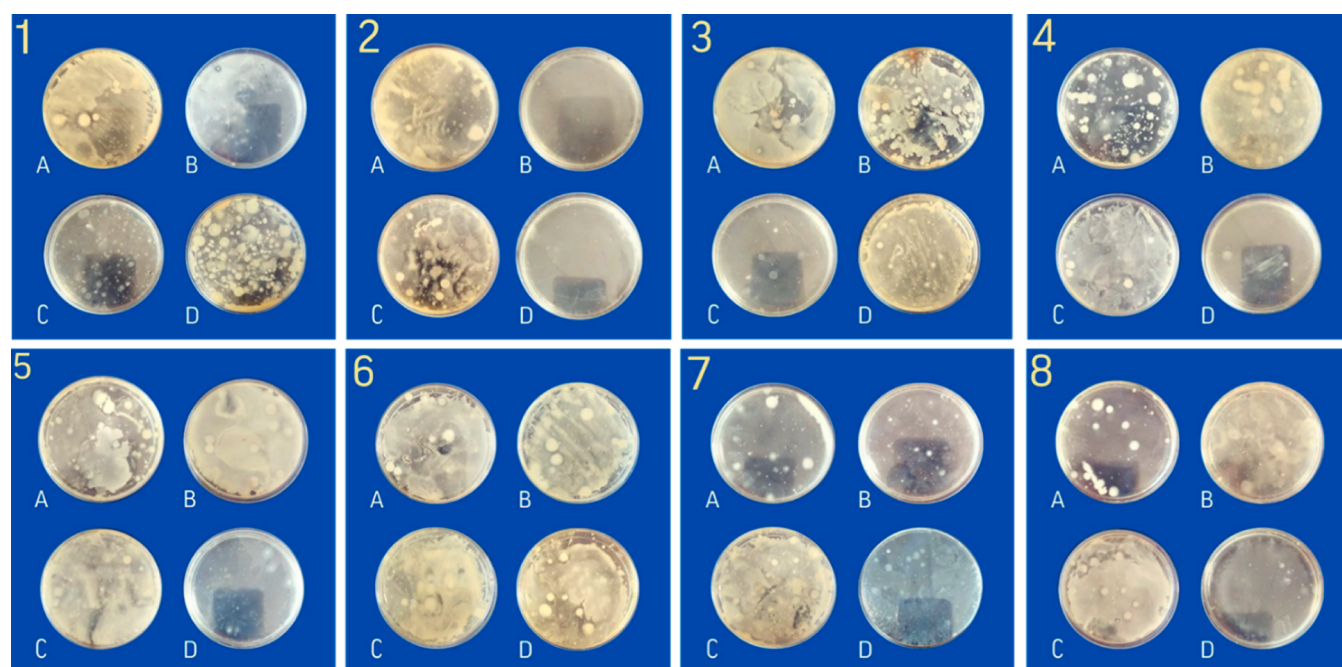
Figure 10. Photographs of Petri dishes with *L. rhamnosus* seeded in agar–agar medium with iron ascorbate threoninate (1), iron ascorbate valinate (2), iron ascorbate methioninate (3), iron ascorbate lysinate (4), iron ascorbate leucinate (5), iron ascorbate phenylalaninate (6), iron ascorbate isoleucinate (7), and iron ascorbate tryptophanate (8) at different concentrations: 0.05 mol/L (A), 0.005 mol/L (B), 0.0005 mol/L (C), and 0.00005 mol/L (D).

Table 8. Effect of AsA-Fe-AmA Triple Chelate Complexes on *L. rhamnosus*

AsA-Fe-AmA triple chelate complexes	CFU, × 106 in 1 mL			
	0.05 mol/L	0.005 mol/L	0.0005 mol/L	0.00005 mol/L
iron ascorbate threoninate	0.82	1.10	1.54	1.42
iron ascorbate valinate	0.48	0	0.79	0
iron ascorbate methioninate	0.80	1.43	1.55	1.44
iron ascorbate lysinate	0.75	1.12	1.50	1.46
iron ascorbate leucinate	0.76	0.68	1.56	1.38
iron ascorbate phenylalaninate	0.80	0.95	0.87	1.23
iron ascorbate isoleucinate	0.79	0.89	1.17	1.20
iron ascorbate tryptophanate	0.77	1.24	1.25	1.21
control	1.2			

can increase milk fermentation while fortifying the end product with iron.

3.8. Production of Fermented Milk Product Fortified with AsA-Fe-AmA Triple Chelate Complexes.

The fermented dairy product samples fortified with AsA-Fe-AmA

triple chelate complexes underwent testing for TA, pH, and viscosity. The results are shown in Table 9.

Table 9 illustrates that fortifying fermented milk products with AsA-Fe-AmA triple chelate complexes resulted in a significant increase in TA across the samples. Among them, the sample containing iron ascorbate tryptophanate had the

Table 9. Physical and Chemical Properties of Fermented Milk Products Fortified with AsA-Fe-AmA Triple Chelate Complexes

AsA-Fe-AmA triple chelate complexes	titrated acidity, °T[a]	pH[a]	viscosity, Pa·s[a]
iron ascorbate lysinate	66 ± 1	4.39 ± 0.05	1896 ± 132
iron ascorbate isoleucinate	104 ± 1	4.37 ± 0.05	2313 ± 161
iron ascorbate leucinate	104 ± 1	4.40 ± 0.05	2075 ± 145
iron ascorbate methioninate	67 ± 1	4.38 ± 0.05	2018 ± 142
iron ascorbate valinate	57 ± 1	4.39 ± 0.05	1979 ± 139
iron ascorbate phenylalaninate	126 ± 1	4.38 ± 0.05	2030 ± 141
iron ascorbate tryptophanate	193 ± 1	4.35 ± 0.05	2027 ± 139
iron ascorbate threoninate	157 ± 1	4.38 ± 0.05	1790 ± 125
iron(II) sulfate	145 ± 1	4.40 ± 0.05	1810 ± 127
control sample	56 ± 1	4.39 ± 0.05	1809 ± 129

[a]X ± standard error of device (N = 3).

Table 10. Sensory Characteristics of Fermented Milk Product Fortified with AsA-Fe-AmA Triple Chelate Complexes

sample	general description	total value[a]
iron(II) sulfate	presence of lumps, creamy color, whey odor and taste, lumpy structure, fluid	4.00
iron ascorbate lysinate	presence of lumps, creamy color, whey smell and taste, lumpy structure, fluid	4.40
iron ascorbate valinate	presence of lumps, creamy color, whey smell and taste, lumpy structure, fluid	3.40
iron ascorbate isoleucinate	presence of lumps, creamy color, whey smell and taste, lumpy structure, fluid	4.00
iron ascorbate threoninate	presence of lumps, creamy color, whey smell and taste, lumpy structure, fluid	3.35
iron ascorbate methioninate	lumps-free, creamy color, uncharacteristic odor and taste, homogeneous fluid structure	3.30
iron ascorbate tryptophanate	presence of lumps, creamy color, whey smell and taste, lumpy structure, fluid	3.50
iron ascorbate phenylalaninate	lumps-free, creamy color, uncharacteristic odor and taste, homogeneous fluid structure	3.25
iron ascorbate leucinate	presence of lumps, creamy color, whey smell and taste, lumpy structure, fluid	4.00
control sample	presence of lumps, creamy color, whey smell and taste, lumpy structure, fluid	4.00

[a]weighted average value (N = 10).

highest TA value (193 °T). Interestingly, the pH of the samples remained unaffected in AsA-Fe-AmA triple chelate complexes. There was a minimal change in viscosity compared to the control sample, except for samples with iron ascorbate isoleucinate, which increased to 504 Pa·s. The established trend of increasing TA and slightly increasing viscosity aligns with the previous findings in studies involving milk, yogurt, cheese, and similar products.[83,88,89]

The sensory assessment of a fermented milk product enriched with AsA-Fe-AmA triple chelate complexes was conducted at the end of the experiment (Table 10).

The sensory evaluation revealed that fermented milk product samples fortified with AsA-Fe-AmA triple chelate complexes primarily exhibited a creamy color, lumps in the composition, whey odor and taste, lumpiness, and a fluid structure, except for those fortified with iron ascorbate phenylalaninate and iron ascorbate methioninate, which received the lowest total value. It is crucial to highlight samples fortified with iron ascorbate phenylalanine and iron ascorbate methioninate, which emitted a distinct odor characteristic of the amino acids phenylalanine and methionine. The overall value was rather low in samples containing iron ascorbate threoninate, iron ascorbate valinate, and iron ascorbate tryptophanate. Sensory acceptance plays a vital role in developing new food products as it directly influences customer behavior.[88,89]

The results revealed that iron ascorbate lysinate boosts the growth and development of lactic acid bacteria *L. rhamnosus*, possesses strong antioxidant activities, and maintains the dispersed characteristics of the dispersed phase of milk. Fortification of fermented milk product with iron ascorbate lysinate had no negative effect on taste and odor of the resulting product. As a result, based on these findings, iron ascorbate lysinate was chosen as the optimal AsA-Fe-AmA triple chelate complex for fortifying fermented milk products and can be further investigated as a potential molecule for addressing iron deficiency anemia food through food fortification.[90,91]

In summary, the developed triple chelate complexes have been observed to be effective for the fortification of dairy and fermented milk products, thereby preventing ID and ID anemia. It is noteworthy that these complexes can be used not only in the food industry but also in medicine, pharmacy, and veterinary as dietary supplements for the prevention of ID and ID anemia in humans and animals.

4. CONCLUSIONS

This work marks the first study of novel AsA-Fe-AmA triple chelate complexes. Analysis of their optical properties revealed that all of the collected samples of AsA-Fe-AmA triple chelate complexes exhibit a maximum absorption band in the absorption spectrum between 552 and 567 nm. Computed quantum chemical modeling highlighted molecular interactions involving the amino and carboxyl groups of AmA and hydroxyl groups linked to the C2 and C3 carbon atoms of AsA. FTIR spectroscopy elucidated the mechanism of AsA-Fe-AmA triple chelate complexes. A study of the stability of the AsA-Fe-AmA triple chelate complexes at various technical parameters suggested their suitability for fortifying food items with pH 3—7, not subjected to heat treatment exceeding 75 °C for more than 15 min.

It is important to note that AsA-Fe-AmA triple chelate complexes increase serum iron levels in the rat model with ID anemia within 24 h following a single oral administration to reference values. The in vivo investigation demonstrated that the addition of 2 mL of compound increased the iron content by 14.0 mmol/L. This finding suggests that complex fermented

milk products fortified with this compound can effectively be used to prevent iron deficiency and iron deficiency anemia.

The antioxidant activity of fortified milk was assessed, and it was discovered that the incorporation of AsA-Fe-AmA triple chelate complexes led to an overall increase in the antioxidant activity. Through sensory evaluation, it was determined that iron ascorbate tryptophanate and iron ascorbate phenylalaninate are ideal in terms of sensory acceptance, suggesting them a potential candidate substance for food fortification in iron deficiency anemia.

Microbiological research revealed that iron ascorbate threoninate, iron ascorbate methioninate, iron ascorbate lysinate, and iron ascorbate tryptophanate have a positive effect on the growth and development of *L. rhamnosus* lactic acid cultures at concentrations of 0.0005 mol/L or lower. These findings are significant, as they indicate that the complexes not only enhance milk fermentation but also fortify the final product with iron. It was found that fortified fermented milk product has a titratable acidity of 67 ± 1 °T, pH of 4.38 ± 0.05, and viscosity of 2018 ± 142 Pa s. Among the AsA-Fe-AmA triple chelate complexes studied, iron ascorbate lysinate emerged as the most effective complex, demonstrating potential for dietary fortification in iron deficiency anemia.

ASSOCIATED CONTENT

Supporting Information

The Supporting Information is available free of charge at https://pubs.acs.org/doi/10.1021/acsomega.4c02664.

Results of quantum chemical modeling of 60 molecular complexes, IR spectra of ascorbic acid and amino acids, and ternary surfaces of dependences of changes in the optical density of samples on technological parameters of temperature and exposure time or pH and temperature (PDF)

AUTHOR INFORMATION

Corresponding Authors

Faten Abdo Hassan — *Faculty of Science, Department of Microbiology, Taiz University, Taiz 9674, Yemen;* orcid.org/0000-0002-0233-5539; Email: fatenhassan@taiz.edu.ye

Mohammad Ali Shariati — *Scientific Department, Semey Branch of the Kazakh Research Institute of Processing and Food Industry, Almaty 050060, Kazakhstan;* Email: shariatymohammadali@gmail.com

Authors

Alexey Gvozdenko — *Physical and Technical Faculty, North-Caucasus Federal University, Stavropol 355017, Russia*

Andrey Blinov — *Physical and Technical Faculty, North-Caucasus Federal University, Stavropol 355017, Russia*

Alexey Golik — *Physical and Technical Faculty, North-Caucasus Federal University, Stavropol 355017, Russia*

Zafar Rekhman — *Physical and Technical Faculty, North-Caucasus Federal University, Stavropol 355017, Russia*

Andrey Nagdalian — *Laboratory of Food and Industrial Biotechnology, North-Caucasus Federal University, Stavropol 355017, Russia*

Dionis Filippov — *Physical and Technical Faculty, North-Caucasus Federal University, Stavropol 355017, Russia*

Alina Askerova — *Laboratory of Food and Industrial Biotechnology, North-Caucasus Federal University, Stavropol 355017, Russia*

Nikita Bocharov — *Physical and Technical Faculty, North-Caucasus Federal University, Stavropol 355017, Russia*

Elena Kastarnova — *Eterinary Faculty, Stavropol Sate Agrarian University, Stavropol 355017, Russia;* orcid.org/0000-0003-2843-2473

Ammar AL-Farga — *Department of Biochemistry, College of Science, University of Jeddah, Jeddah 21577, Saudi Arabia*

Complete contact information is available at: https://pubs.acs.org/10.1021/acsomega.4c02664

Notes

The authors declare no competing financial interest.

Limitations: The current study showed promising results on the use of AsA-Fe-AmA triple chelate complexes in fermented dairy products' fortification, as well as revealed a gap in full understanding of the activity of developed complexes. Thus, in vivo experiments showed the need for 30 days of research on rat model with ID anemia to understand how AsA-Fe-AmA triple chelate complexes exert an influence on hemoglobin, erythrocyte, and hematocrit levels in animals' blood. Before the realization of fortified fermented dairy products, in vivo studies should be carried out with laboratory animals and human volunteers to assess AsA-Fe-AmA triple chelate complexes for potential toxic effect, digestibility, and influence on immunity indicators. Further research should also provide a understanding of more accurate concentrations of AsA-Fe-AmA triple chelate complexes needed for fermented dairy products' fortification. Further sensory evaluation using a hedonic test should be carried out with at least 50 untrained panelists to make the results more objective and cleaner.

ACKNOWLEDGMENTS

REFERENCES

(1) Ali, A. A. H. Overview of the Vital Roles of Macro Minerals in the Human Body. *J. Trace Elem. Miner.* **2023**, *4*, 100076.

(2) Gombart, A. F.; Pierre, A.; Maggini, S. A Review of Micronutrients and the Immune System-Working in Harmony to Reduce the Risk of Infection. *Nutrients* **2020**, *12*, 236.

(3) Hatch-McChesney, A.; Lieberman, H. R. Iodine and Iodine Deficiency: A Comprehensive Review of a Re-Emerging Issue. *Nutrients* **2022**, *14*, 3474.

(4) Morton, C. M.; Pullabhotla, H.; Bevis, L.; Lobell, D. B. Soil Micronutrients Linked to Human Health in India. *Sci. Rep.* **2023**, *13*, 13591.

(5) Amrein, K.; Scherkl, M.; Hoffmann, M.; Neuwersch-Sommeregger, S.; Köstenberger, M.; Tmava Berisha, A.; Martucci, G.; Pilz, S.; Malle, O. Vitamin D Deficiency 2.0: An Update on the Current Status Worldwide. *Eur. J. Clin. Nutr.* **2020**, *74*, 1498−1513.

(6) Kanasaki, K.; Kumagai, A. The Impact of Micronutrient Deficiency on Pregnancy Complications and Development Origin of Health and Disease. *J. Obstet. Gynaecol. Res.* **2021**, *47*, 1965−1972.

(7) Ceolin, C.; Papa, M. V.; De Rui, M.; Devita, M.; Sergi, G.; Coin, A. Micronutrient Deficiency and Its Potential Role in Delirium Onset in Older Adults: A Systematic Review. *J. Nutr. Heal. Aging* **2023**, *27* (9), 785−790.

(8) Stevens, G. A.; Beal, T.; Mbuya, M. N. N.; Luo, H.; Neufeld, L. M.; Addo, O. Y.; Adu-Afarwuah, S.; Alayón, S.; Bhutta, Z.; Brown, K. H.;

Jefferds, M. E.; Engle-Stone, R.; Fawzi, W.; Hess, S. Y.; Johnston, R.; Katz, J.; Krasevec, J.; McDonald, C. M.; Mei, Z.; Osendarp, S.; Paciorek, C. J.; Petry, N.; Pfeiffer, C. M.; Ramirez-Luzuriaga, M. J.; Rogers, L. M.; Rohner, F.; Sethi, V.; Suchdev, P. S.; Tessema, M.; Villapando, S.; Wieringa, F. T.; Williams, A. M.; Woldeyahannes, M.; Young, M. F. Micronutrient Deficiencies among Preschool-Aged Children and Women of Reproductive Age Worldwide: A Pooled Analysis of Individual-Level Data from Population-Representative Surveys. *Lancet Global Health* **2022**, *10* (11), E1590−E1599.

(9) Baugreet, S.; Hamill, R. M.; Kerry, J. P.; McCarthy, S. N. Mitigating Nutrition and Health Deficiencies in Older Adults: A Role for Food Innovation? *J. Food Sci.* **2017**, *82* (4), 848−855.

(10) Littlejohn, P. T.; Metcalfe-Roach, A.; Cardenas Poire, E.; Holani, R.; Bar-Yoseph, H.; Fan, Y. M.; Woodward, S. E.; Finlay, B. B. Multiple Micronutrient Deficiencies in Early Life Cause Multi-Kingdom Alterations in the Gut Microbiome and Intrinsic Antibiotic Resistance Genes in Mice. *Nat. Microbiol.* **2023**, *8* (12), 2392−2405.

(11) Cashman, K. D. Vitamin D Deficiency: Defining, Prevalence, Causes, and Strategies of Addressing. *Calcif. Tissue Int.* **2020**, *106*, 14−29.

(12) Surman, S. L.; Penkert, R. R.; Sealy, R. E.; Jones, B. G.; Marion, T. N.; Vogel, P.; Hurwitz, J. L. Consequences of Vitamin a Deficiency: Immunoglobulin Dysregulation, Squamous Cell Metaplasia, Infectious Disease, and Death. *Int. J. Mol. Sci.* **2020**, *21*, 5570.

(13) Mrowicka, M.; Mrowicki, J.; Dragan, G.; Majsterek, I. The Importance of Thiamine (Vitamin B1) in Humans. *Biosci. Rep.* **2023**, *43* (10), 1−18.

(14) Gernand, A. D.; Schulze, K. J.; Stewart, C. P.; West, K. P.; Christian, P. Micronutrient Deficiencies in Pregnancy Worldwide: Health Effects and Prevention. *Nat. Rev. Endocrinol.* **2016**, *12*, 274−289.

(15) Kinyoki, D.; Osgood-Zimmerman, A. E.; Bhattacharjee, N. V.; Schaeffer, L. E.; Lazzar-Atwood, A.; Lu, D.; Ewald, S. B.; Donkers, K. M.; Letourneau, I. D.; Collison, M.; et al. Anemia Prevalence in Women of Reproductive Age in Low- and Middle-Income Countries between 2000 and 2018. *Nat. Med.* **2021**, *27* (10), 1761−1782.

(16) Cacoub, P.; Nicolas, G.; Peoc'h, K. Iron Deficiency Markers in Patients Undergoing Iron Replacement Therapy: A 9-Year Retrospective Real-World Evidence Study Using Healthcare Databases. *Sci. Rep.* **2020**, *10* (1), 14983.

(17) Gottwald, E. M.; Schuh, C. D.; Drücker, P.; Haenni, D.; Pearson, A.; Ghazi, S.; Bugarski, M.; Polesel, M.; Duss, M.; Landau, E. M.; Kaech, A.; Ziegler, U.; Lundby, A. K. M.; Lundby, C.; Dittrich, P. S.; Hall, A. M. The Iron Chelator Deferasirox Causes Severe Mitochondrial Swelling without Depolarization Due to a Specific Effect on Inner Membrane Permeability. *Sci. Rep.* **2020**, *10*, 1577.

(18) Li, H.; Zhao, H.; Hao, S.; Shang, L.; Wu, J.; Song, C.; Meyron-Holtz, E. G.; Qiao, T.; Li, K. Iron Regulatory Protein Deficiency Compromises Mitochondrial Function in Murine Embryonic Fibroblasts. *Sci. Rep.* **2018**, *8*, 5118.

(19) Fang, X.; Ardehali, H.; Min, J.; Wang, F. The Molecular and Metabolic Landscape of Iron and Ferroptosis in Cardiovascular Disease. *Nat. Rev. Cardiol.* **2023**, *20*, 7−23.

(20) Neidlein, S.; Wirth, R.; Pourhassan, M. Iron Deficiency, Fatigue and Muscle Strength and Function in Older Hospitalized Patients. *Eur. J. Clin. Nutr.* **2021**, *75*, 456−463.

(21) Pasricha, S. R.; Tye-Din, J.; Muckenthaler, M. U.; Swinkels, D. W. Iron Deficiency. *Lancet* **2021**, *397*, 233−248.

(22) Mirza, F. G.; Abdul-Kadir, R.; Breymann, C.; Fraser, I. S.; Taher, A. Impact and management of iron deficiency and iron deficiency anemia in women's health. *Expert Rev. Hematol.* **2018**, *11* (9), 727−736.

(23) Christian, P. Anemia in Women—an Intractable Problem That Requires Innovative Solutions. *Nat. Med.* **2021**, *27* (10), 1675−1677.

(24) WHO. Anemia. 2023. https://www.who.int/news-room/fact-sheets/detail/anaemia (accessed Feb 26, 2024).

(25) Stevens, G. A.; Paciorek, C. J.; Flores-Urrutia, M. C.; Borghi, E.; Namaste, S.; Wirth, J. P.; Suchdev, P. S.; Ezzati, M.; Rohner, F.; Flaxman, S. R.; Rogers, L. M. National, Regional, and Global Estimates of Anaemia by Severity in Women and Children for 2000−19: A Pooled

Analysis of Population-Representative Data. *Lancet Global Health* **2022**, *10* (5), E627−E639.

(26) Hasan, M. M.; Soares Magalhaes, R. J.; Garnett, S. P.; Fatima, Y.; Tariqujjaman, M.; Pervin, S.; Ahmed, S.; Mamun, A. A. Anaemia in Women of Reproductive Age in Low-and Middle-Income Countries: Progress towards the 2025 Global Nutrition Target. *Bull. World Health Organ.* **2022**, *100*, 196−204.

(27) WHO. Global Nutrition Targets 2025: Policy Brief Series. https://www.who.int/publications-detail-redirect/WHO-NMH-NHD-14.2 (accessed Feb 26, 2024).

(28) Cappellini, M. D.; Musallam, K. M.; Taher, A. T. Iron Deficiency Anaemia Revisited. *J. Intern. Med.* **2020**, *287*, 153−170.

(29) Nairz, M.; Weiss, G. Iron in Infection and Immunity. *Mol. Aspects Med.* **2020**, *75*, 100864.

(30) Phipps, O.; Brookes, M. J.; Al-Hassi, H. O. Iron Deficiency, Immunology, and Colorectal Cancer. *Nutr. Rev.* **2021**, *79*, 88−97.

(31) Bathla, S.; Arora, S. Prevalence and Approaches to Manage Iron Deficiency Anemia (IDA). *Crit. Rev. Food Sci. Nutr.* **2022**, *62*, 8815−8828.

(32) Nair, M. K.; Augustine, L. F.; Konapur, A. Food-Based Interventions to Modify Diet Quality and Diversity to Address Multiple Micronutrient Deficiency. *Front. Public Health* **2016**, *3*, 277.

(33) Kazemi-Taskooh, Z.; Varidi, M. Food-Based Iron Delivery Systems: A Review. *Trends Food Sci. Technol.* **2021**, *116*, 75−89.

(34) Fernández-Lázaro, D.; Mielgo-Ayuso, J.; Córdova Martínez, A.; Seco-Calvo, J. Iron and Physical Activity: Bioavailability Enhancers, Properties of Black Pepper (Bioperine®) and Potential Applications. *Nutrients* **2020**, *12* (6), 1886.

(35) Shapterhasmi, T.; Palani, N.; Velusamy, M.; Bhuvanesh, N. S. P.; Sundaravel, K.; Easwaramoorthi, S. Iron(III) Complexes of Pyrrolidine and Piperidine Appended Tridentate 3N Donor Ligands as Models for Catechol Dioxygenase Enzymes. *Inorg. Chim. Acta* **2022**, *537*, 120924.

(36) Feng, Y.; Wassie, T.; Wu, Y.; Wu, X. Advances on Novel Iron Saccharide-Iron (III) Complexes as Nutritional Supplements. *Crit. Rev. Food Sci. Nutr.* **2023**, 1−17.

(37) Yang, H.; Zang, X.; Jin, X.; Chen, J.; Lv, Y.; Lv, Z. Efficacy of Polysaccharide Iron Complex in IDA Rats: A Comparative Study with Iron Protein Succinylate and Ferrous Succinate. *Biomed. Pharmacother.* **2024**, *170*, 115991.

(38) Tolkien, Z.; Stecher, L.; Mander, A. P.; Pereira, D. I. A.; Powell, J. J. Ferrous Sulfate Supplementation Causes Significant Gastrointestinal Side-Effects in Adults: A Systematic Review and Meta-Analysis. *PLoS One* **2015**, *10* (2), No. e0117383.

(39) McMillen, S. A.; Dean, R.; Dihardja, E.; Ji, P.; Lönnerdal, B. Benefits and Risks of Early Life Iron Supplementation. *Nutrients* **2022**, *14* (20), 4380.

(40) Malesza, I. J.; Bartkowiak-Wieczorek, J.; Winkler-Galicki, J.; Nowicka, A.; Dzięciołowska, D.; Błaszczyk, M.; Gajniak, P.; Słowińska, K.; Niepolski, L.; Walkowiak, J.; Mądry, E. The Dark Side of Iron: The Relationship between Iron, Inflammation and Gut Microbiota in Selected Diseases Associated with Iron Deficiency Anaemia—A Narrative Review. *Nutrients* **2022**, *14* (17), 3478.

(41) Di Vincenzo, F.; Del Gaudio, A.; Petito, V.; Lopetuso, L. R.; Scaldaferri, F. Gut Microbiota, Intestinal Permeability, and Systemic Inflammation: A Narrative Review. *Int. Emerg. Med.* **2023**, *19*, 275−293.

(42) Ellermann, M.; Gharaibeh, R. Z.; Maharshak, N.; Peréz-Chanona, E.; Jobin, C.; Carroll, I. M.; Arthur, J. C.; Plevy, S. E.; Fodor, A. A.; Brouwer, C. R.; Sartor, R. B. Dietary Iron Variably Modulates Assembly of the Intestinal Microbiota in Colitis-Resistant and Colitis-Susceptible Mice. *Gut Microbes* **2020**, *11* (1), 32−50.

(43) Cross, J. H.; Bradbury, R. S.; Fulford, A. J.; Jallow, A. T.; Wegmüller, R.; Prentice, A. M.; Cerami, C. Oral Iron Acutely Elevates Bacterial Growth in Human Serum. *Sci. Rep.* **2015**, *5* (1), 16670.

(44) Moksnes, M. R.; Graham, S. E.; Wu, K.-H.; Hansen, A. F.; Gagliano Taliun, S. A.; Zhou, W.; Thorstensen, K.; Fritsche, L. G.; Gill, D.; Mason, A.; Cucca, F.; Schlessinger, D.; Abecasis, G. R.; Burgess, S.; Åsvold, B. O.; Nielsen, J. B.; Hveem, K.; Willer, C. J.; Brumpton, B. M. Genome-Wide Meta-Analysis of Iron Status Biomarkers and the Effect

of Iron on All-Cause Mortality in HUNT. *Commun. Biol.* **2022**, *5* (1), 591.

(45) Zhang, S.; Xin, W.; Anderson, G. J.; Li, R.; Gao, L.; Chen, S.; Zhao, J.; Liu, S. Double-Edge Sword Roles of Iron in Driving Energy Production versus Instigating Ferroptosis. *Cell Death Dis.* **2022**, *13* (1), 40.

(46) Cherry, K. Intravenous versus Oral Iron Supplementation for Iron-Deficiency Anemia. *Nat. Clin. Pract. Gastroenterol. Hepatol.* **2006**, *3* (2), 63.

(47) Bloor, S. R.; Schutte, R.; Hobson, A. R. Oral Iron Supplementation—Gastrointestinal Side Effects and the Impact on the Gut Microbiota. *Microbiol. Res. (Pavia).* **2021**, *12* (2), 491−502.

(48) Kumar, A.; Brookes, M. J. Iron Therapy in Inflammatory Bowel Disease. *Nutrients* **2020**, *12* (11), 3478.

(49) Kontoghiorghes, G. J.; Kolnagou, A.; Kontoghiorghe, C. N.; Mourouzidis, L.; Timoshnikov, V. A.; Polyakov, N. E. Trying to Solve the Puzzle of the Interaction of Ascorbic Acid and Iron: Redox, Chelation and Therapeutic Implications. *Medicines* **2020**, *7* (8), 45.

(50) Shen, J.; Griffiths, P. T.; Campbell, S. J.; Utinger, B.; Kalberer, M.; Paulson, S. E. Ascorbate Oxidation by Iron, Copper and Reactive Oxygen Species: Review, Model Development, and Derivation of Key Rate Constants. *Sci. Rep.* **2021**, *11* (1), 7417.

(51) Noubactep, C.; Kenmogne-Tchidjo, J. F.; Vollmer, S. Iron-Fortified Water: A New Approach for Reducing Iron Deficiency Anemia in Resource-Constrained Settings. *Sci. Rep.* **2023**, *13* (1), 13565.

(52) Cian, R. E.; Proaño, J. L.; Salgado, P. R.; Mauri, A. N.; Drago, S. R. High Iron Bioaccessibility from Co-Microencapsulated Iron/Ascorbic Acid Using Chelating Polypeptides from Brewers' Spent Grain Protein as Wall Material. *LWT* **2021**, *139*, 110579.

(53) Blinov, A.; Gvozdenko, A.; Golik, A.; Maslova, A.; Verevkina, M. Synthesis and Stability Study of Iron(II) Ascorbatolizinate. In *AIP Conference Proceedings*; 2023; Vol. *2931*, p 060004. .

(54) Blinov, A. V.; Siddiqui, S. A.; Blinova, A. A.; Khramtsov, A. G.; Oboturova, N. P.; NagdalianSimonovIbrahim, A. A.A. N. S. A.; Simonov, A. N.; Ibrahim, S. A. Analysis of the Dispersed Composition of Milk Using Photon Correlation Spectroscopy. *J. Food Compos. Anal.* **2022**, *108*, 104414.

(55) An, G.; Park, S.; Ha, J. The Enhancement Effect of Mungbean on the Physical, Functional, and Sensory Characteristics of Soy Yoghurt. *Sci. Rep.* **2024**, *14* (1), 3684.

(56) Piskov, S.; Timchenko, L.; Avanesyan, S.; Siddiqui, S. A.; Sizonenko, M.; Kurchenko, V.; Rzhepakovsky, I.; Blinov, A.; Nagdalian, A.; Shariati, M. A.; Ibrahim, S. A. A Comparative Study on the Structural Properties and Lipid Profile of Mushroom (Pleurotus Ostreatus) Powder Obtained by Different Drying Methods. *Agriculture* **2022**, *12* (10), 1590.

(57) ISO 22935−2:2023. Milk and Milk Products. Sensory Analysis. Part 2: Recommended Methods for Sensory Evaluation. Https://Www.Iso.Org/Standard/84532.Html (accessed March 1, 2024).

(58) Alonso-Roman, R.; Last, A.; Mirhakkak, M. H.; Sprague, J. L.; Möller, L.; Großmann, P.; Graf, K.; Gratz, R.; Mogavero, S.; Vylkova, S.; Panagiotou, G.; Schäuble, S.; Hube, B.; Gresnigt, M. S. Lactobacillus Rhamnosus Colonisation Antagonizes Candida Albicans by Forcing Metabolic Adaptations That Compromise Pathogenicity. *Nat. Commun.* **2022**, *13* (1), 3192.

(59) Sebastián-Nicolas, J. L.; Contreras-López, E.; Ramírez-Godínez, J.; Cruz-Guerrero, A. E.; Rodríguez-Serrano, G. M.; Añorve-Morga, J.; Jaimez-Ordaz, J.; Castañeda-Ovando, A.; Pérez-Escalante, E.; Ayala-Niño, A.; González-Olivares, L. G. Milk Fermentation by Lacticaseibacillus Rhamnosus GG and Streptococcus Thermophilus SY-102: Proteolytic Profile and ACE-Inhibitory Activity. *Fermentation* **2021**, *7* (4), 215.

(60) Niedzielski, P.; Zielinska-Dawidziak, M.; Kozak, L.; Kowalewski, P.; Szlachetka, B.; Zalicka, S.; Wachowiak, W. Determination of Iron Species in Samples of Iron-Fortified Food. *Food Anal. Methods* **2014**, *7*, 2023−2032.

(61) Majka, G.; Śpiewak, K.; Kurpiewska, K.; Heczko, P.; Stochel, G.; Strus, M.; Brindell, M. A High-Throughput Method for the

Quantification of Iron Saturation in Lactoferrin Preparations. *Anal. Bioanal. Chem.* **2013**, *405*, 5191−5200.

(62) Bogojeski, M.; Vogt-Maranto, L.; Tuckerman, M. E.; Müller, K. R.; Burke, K. Quantum Chemical Accuracy from Density Functional Approximations via Machine Learning. *Nat. Commun.* **2020**, *11* (1), 5223.

(63) Lindoy, L. P.; Mandal, A.; Reichman, D. R. Quantum Dynamical Effects of Vibrational Strong Coupling in Chemical Reactivity. *Nat. Commun.* **2023**, *14* (1), 2733.

(64) Gujarati, T. P.; Motta, M.; Friedhoff, T. N.; Rice, J. E.; Nguyen, N.; Barkoutsos, P. K.; Thompson, R. J.; Smith, T.; Kagele, M.; Brei, M.; Jones, B. A.; Williams, K. Quantum Computation of Reactions on Surfaces Using Local Embedding. *npj Quantum Inf.* **2023**, *9* (1), 88.

(65) Khamespanah, F.; Marx, M.; Crochet, D. B.; Pokharel, U. R.; Fronczek, F. R.; Maverick, A. W.; Beller, M. Oxalate Production via Oxidation of Ascorbate Rather than Reduction of Carbon Dioxide. *Nat. Commun.* **2021**, *12* (1), 1997.

(66) Kim, J.; Lee, T.; Jung, H. D.; Kim, M.; Eo, J.; Kang, B.; Jung, H.; Park, J.; Bae, D.; Lee, Y.; Park, S.; Kim, W.; Back, S.; Lee, Y.; Nam, D. H. Vitamin C-Induced CO_2 Capture Enables High-Rate Ethylene Production in CO_2 Electroreduction. *Nat. Commun.* **2024**, *15* (1), 192.

(67) Barreto, M. S. C.; Elzinga, E. J.; Alleoni, L. R. F. The Molecular Insights into Protein Adsorption on Hematite Surface Disclosed by In-Situ ATR-FTIR/2D-COS Study. *Sci. Rep.* **2020**, *10* (1), 13441.

(68) Mirzaee, S.; Shayesteh, S. F. Ultrasound Induced Strain in Ultrasmall $CoFe_2O_4$@polyvinyl Alcohol Nanocomposites. *Ultrason. Sonochem.* **2018**, *40*, 583−586.

(69) Andris, E.; Navrátil, R.; Jašík, J.; Sabenya, G.; Costas, M.; Srnec, M.; Roithová, J. Detection of Indistinct Fe-N Stretching Bands in Iron(V) Nitrides by Photodissociation Spectroscopy. *Chem.—A Eur. J.* **2018**, *24* (20), 5078−5081.

(70) Gilliard Nkhata, S. Iron Fortification of Yogurt and Pasteurized Milk. *J. Nutr. Heal. Food Sci.* **2015**, *3* (3), 1−12.

(71) Darwish, A. M. G.; Soliman, T. N.; Elhendy, H. A.; El-Kholy, W. M. Nano-Encapsulated Iron and Folic Acid-Fortified Functional Yogurt Enhance Anemia in Albino Rats. *Front. Nutr.* **2021**, *8*, 654624.

(72) Ben-Ishay, N.; Oknin, H.; Steinberg, D.; Berkovich, Z.; Reifen, R.; Shemesh, M. Enrichment of Milk with Magnesium Provides Healthier and Safer Dairy Products. *npj Biofilms Microbiomes* **2017**, *3* (1), 24.

(73) Smialowska, A.; Matia-Merino, L.; Carr, A. J. Assessing the Iron Chelation Capacity of Goat Casein Digest Isolates. *J. Dairy Sci.* **2017**, *100* (4), 2553−2563.

(74) Johns, P. W.; Strozier, D. C.; McKenna, R. J.; Veldhuis, J.; Weber, L. E.; Thompson, J. J. Evaluations of Protein-Metal Association in Nutritional Products. *Int. Dairy J.* **2021**, *114*, 104912.

(75) Ghorbani, S.; Shekarforoush, S. S.; Niakousari, M.; Gheisari, H. R.; Janipour, R. Formulation and Assessing Characteristics of Probiotic Ice Cream Fortified with Free and Encapsulated Iron. *J. Food Meas. Charact.* **2023**, *17* (1), 499−507.

(76) Balakirev, N. A. iron deficiency anemia in laboratory rats to be used as an experimental model for farmed fur-bearing animals. *S-kh. Biol.* **2022**, *57*, 718−729.

(77) He, H.; Huang, Q.; Liu, C.; Jia, S.; Wang, Y.; An, F.; Song, H. Effectiveness of AOS-Iron on Iron Deficiency Anemia in Rats. *RSC Adv.* **2019**, *9*, 5053−5063.

(78) Blinov, A. V.; Siddiqui, S. A.; Nagdalian, A. A.; Blinova, A. A.; Gvozdenko, A. A.; Raffa, V. V.; Oboturova, N. P.; Golik, A. B.; Maglakelidze, D. G.; Ibrahim, S. A. Investigation of the Influence of Zinc-Containing Compounds on the Components of the Colloidal Phase of Milk. *Arab. J. Chem.* **2021**, *14* (7), 103229.

(79) Khan, I. T.; Nadeem, M.; Imran, M.; Ullah, R.; Ajmal, M.; Jaspal, M. H. Antioxidant Properties of Milk and Dairy Products: A Comprehensive Review of the Current Knowledge. *Lipids Health Dis.* **2019**, *18* (1), 41.

(80) Khan, I. T.; Bule, M.; Ullah, R.; Nadeem, M.; Asif, S.; Niaz, K. The Antioxidant Components of Milk and Their Role in Processing, Ripening, and Storage: Functional Food. *Vet. World* **2019**, *12* (1), 12−33.

(81) Yeh, E. B.; Barbano, D. M.; Drake, M. Vitamin Fortification of Fluid Milk. *J. Food Sci.* **2017**, *82* (4), 856−864.

(82) García, D.; Changanaqui, K.; Vásquez, R. E.; Neira, E.; Espinoza, J. B.; Moran, J. R. V.; Ludeña-Urquizo, F. E.; Alvarado, T. H.; Ramos, M.; Jordan-Suarez, O. B.; Tuesta, T. Heme Iron Fortified Flavored Milk: Quality and Sensory Analysis. *Braz. J. Food Technol.* **2022**, *25*, No. e2020621.

(83) Abdulghani, A. H.; Prakash, S.; Ali, M. Y.; Deeth, H. C. Sensory Evaluation and Storage Stability of UHT Milk Fortified with Iron, Magnesium and Zinc. *Dairy Sci. Technol.* **2015**, *95* (1), 33−46.

(84) Siddique, A.; Park, Y. W. Effect of Iron Fortification on Microstructural, Textural, and Sensory Characteristics of Caprine Milk Cheddar Cheeses under Different Storage Treatments. *J. Dairy Sci.* **2019**, *102* (4), 2890−2902.

(85) Arce, A.; Ustunol, Z. Effect of Microencapsulated Ferrous Sulfate Particle Size on Cheddar Cheese Composition and Quality. *J. Dairy Sci.* **2018**, *101* (8), 6814−6822.

(86) Helmyati, S.; Arsanti Le, L.; Ratna Maya, O.; Wigati, M.; Utami Wisn, S.; Sutriswati, E.; Juffrie, M. Synbiotic Fermented Milk with Tempeh Extract and Iron Fortification: Effect on Antibacterial Activity and Total Enterobacteriaceae. *Am. J. Food Technol.* **2017**, *13* (1), 32−41.

(87) Harouna, S.; Carramiñana, J.; Navarro, F.; Pérez, M.; Calvo, M.; Sánchez, L. Antibacterial Activity of Bovine Milk Lactoferrin on the Emerging Foodborne Pathogen Cronobacter Sakazakii: Effect of Media and Heat Treatment. *Food Control* **2015**, *47*, 520−525.

(88) Banjare, I. S.; Gandhi, K.; Sao, K.; Arora, S.; Pandey, V. Physicochemical Properties and Oxidative Stability of Milk Fortified with Spray-Dried Whey Protein Concentrate-Iron Complex and In Vitro Bioaccessibility of the Added Iron. *Food Technol. Biotechnol.* **2019**, *57* (1), 48−58.

(89) Santillán-Urquiza, E.; Méndez-Rojas, M. Á.; Vélez-Ruiz, J. F. Fortification of Yogurt with Nano and Micro Sized Calcium, Iron and Zinc, Effect on the Physicochemical and Rheological Properties. *LWT* **2017**, *80*, 462−469.

(90) Siegrist, M.; Hartmann, C. Consumer Acceptance of Novel Food Technologies. *Nat. Food* **2020**, *1* (6), 343−350.

(91) Huey, S. L.; Bhargava, A.; Friesen, V. M.; Konieczynski, E. M.; Krisher, J. T.; Mbuya, M. N. N.; Mehta, N. H.; Monterrosa, E.; Nyangaresi, A. M.; Mehta, S. Sensory Acceptability of Biofortified Foods and Food Products: A Systematic Review. *Nutr. Rev.* **2023**, *82* (7), 892−912.